

Electronic Supporting Information for:

Dissimilar-at-boron *N*-BODIPYs: From light-harvesting multichromophoric arrays to CPL-bright *chiral-at-boron* BODIPYs

César Ray,^a Edurne Avellanal-Zaballa,^b Mónica Muñoz-Úbeda,^{c,d} Jessica Colligan,^e Florencio Moreno,^a Gilles Muller,^e Iván López-Montero,^{c,d,f} Jorge Bañuelos,^b Beatriz L. Maroto,^{*,a} and Santiago de la Moya^{*,a}

^a Depto. de Química Orgánica, Facultad de CC. Químicas, Universidad Complutense de Madrid, Ciudad Universitaria s/n, 28040, Madrid, Spain. E-mail: santmoya@ucm.es, belora@ucm.es

^b Depto. de Química Física, Universidad del País Vasco-EHU, Apartado 644, 48080, Bilbao, Spain.

^c Instituto de Investigación Biomédica Hospital Doce de Octubre (imas12), Avda. de Córdoba s/n, 28041, Madrid, Spain.

^d Departamento de Química Física, Facultad de Ciencias Químicas, Universidad Complutense de Madrid, Ciudad Universitaria s/n, 28040, Madrid, Spain.

^e Department of Chemistry, San José State University, San José, CA 95192-0101, USA.

^f Instituto Pluridisciplinar, Universidad Complutense de Madrid, Paseo de Juan XXIII 1, 28040, Madrid, Spain

	Page
S1. General methods, instrumentation and techniques	S1
S2. Synthetic procedures and characterization data	S5
S3. NMR spectra	S12
S4. Tables	S34
S5. Figures	S36
S6. References	S38

S1. General methods, instrumentation and techniques

S1.1 Synthesis

Anhydrous solvents were prepared by distillation over standard drying agents according to common methods. All other solvents were of HPLC grade and were used as provided. Starting chemical substrates and reagents were used as commercially provided unless otherwise indicated. Thin-layer chromatography (TLC) was performed on silica gel plates, and the chromatograms were visualized using UV light ($\lambda = 254$ or 365 nm). Flash column chromatography was performed using silica gel (230-400 mesh). ^1H , ^{13}C and ^{11}B spectra were recorded in CDCl_3 or $\text{DMSO-}d_6$ solution at 20 °C. NMR chemical shifts are expressed in parts per million (δ scale). ^1H and ^{13}C NMR spectra are referenced to residual protons of CDCl_3 ($\delta = 7.26$ and 77.16 ppm, respectively) or $\text{DMSO-}d_6$ ($\delta = 2.50$ and 39.52 ppm, respectively) as internal standard; ^{11}B spectra were referenced to 15% $\text{BF}_3\cdot\text{Et}_2\text{O}$ in CDCl_3 ($\delta = 0.00$ ppm) as external standard. Multiplicity is indicated as follows: s = singlet; d = doublet; t = triplet; q = quartet, m = multiplet and/or multiple resonances; br = broad. Coupling constants (J) are dated in hertz (Hz). The type of carbon (C, CH, CH_2 or CH_3) was assigned by DEPT-135 NMR experiments. Additionally, complex spin-system signals were simulated by using MestRe-C (program version 10.0.1-14719). FTIR spectra were obtained from neat samples using the attenuated total reflection (ATR) technique. High-resolution mass spectrometry (HRMS) was performed by using UPLC sample injection, electrospray ionization (ESI) and hybrid quadrupole time-of-flight mass analyser (QTOF).

S1.2 X-ray diffraction

Intensity data were collected on an Agilent Technologies Super-Nova diffractometer, which was equipped with monochromated $\text{Cu } \alpha$ radiation ($\lambda = 1.54184$ Å) and Atlas CCD detector. Measurement was carried out at $150.01(10)$ K with the help of an Oxford Cryostream 700 PLUS temperature device. Data frames were processed (unit cell determination, analytical absorption correction with face indexing, intensity data integration and correction for Lorentz and polarization effects) using the CrysAlis software package.¹ The structure was solved using Olex22 and refined by full-matrix least-squares with SHELXL-97/14.3 Final geometrical calculations were carried out with Mercury4 and PLATON5,6 as integrated in WinGX.⁷ Crystallographic data (excluding structure factors) for the structure reported in this paper have been deposited with the Cambridge Crystallographic Data Centre as supplementary publication number CCDC-2269820 for **NBDP-7-R** are summarized in Table S3. Copies of the data can be obtained free of charge from <https://www.ccdc.cam.ac.uk/conts/retrieving.html>.

S1.3 Photophysics

Photophysical signatures were recorded using diluted dye solutions (*ca.* 2×10^{-6} M) prepared from a concentrated stock solution in acetone (*ca.* 10^{-3} M), after solvent evaporation under reduced pressure,

and subsequent dilution with the desired solvent of spectroscopic grade. UV-vis absorption and fluorescence spectra were recorded on a Varian (model CARY 4E) spectrophotometer and an Edinburgh Instrument spectrofluorometer (model FLSP 920), respectively. Fluorescence quantum yields (ϕ) were determined from corrected spectra (detector sensibility to the wavelength) by the optically dilute relative method and by using Eq. S1, where I_{exc} is the luminescent intensity at the excitation wavelength, A_{exc} is the absorbance at the excitation wavelength, $\int Id\lambda$ is the numerically integrated intensity from the luminescence spectra, and n is the index of refraction of the solution. The subscripts R and S denote reference and sample, respectively. PM546 in ethanol ($\phi^0 = 0.85$) was used as the reference.

$$\frac{\phi_S}{\phi_R} = \frac{I_{R exc}}{I_{S exc}} \frac{A_{R exc}}{A_{S exc}} \left(\frac{n_S}{n_R} \right)^2 \quad \text{Eq. S1}$$

The aforementioned spectrofluorometer is also equipped with a wavelength-tunable pulsed Fianium laser. Thus, the Time Correlated Single-Photon Counting (TCSPC) technique was used to record the fluorescence decay curves. Fluorescence emission was monitored at the maximum emission wavelength after excitation by the said Fianium at the maximum absorption wavelength. The fluorescence lifetime (τ) was obtained from the slope of the exponential fit of the decay curve, after the deconvolution of the instrumental response signal (recorded by means of a ludox scattering suspension) by means of an iterative method. The goodness of the exponential fit was controlled by statistical parameters (chi-square and the analysis of the residuals). The EET efficiency, Eff_{EET} , was calculated according to Eq. S2, where ϕ^0 and ϕ denote the fluorescence quantum yields of the isolated anthracene donor and of covalently-linked anthracene donor in the EET molecular array, respectively.

$$Eff_{EET} = 100 \cdot [1 - (\phi / \phi^0)] \quad \text{Eq. S2}$$

S1.4. Chiroptics

Optical rotations were recorded on a Perkin-Elmer (model 241) polarimeter (c are expressed in g / 100 mL).

Electronic Circular Dichroism (ECD) spectra were recorded on a Jasco (model J-715) spectropolarimeter using standard quartz cells of 1 cm optical-path length in chloroform solution, unless otherwise indicated, at a dye concentration of *ca.* 5×10^{-6} M.

Circularly polarized luminescence (CPL) and total luminescence spectra were recorded at 295 K in degassed cyclohexane (nitrogen was bubbled into the solution), at a dye concentration of *ca.* 2×10^{-3} M, upon excitation at *ca.* 515 nm on an instrument described previously,² operating in a differential photon-counting mode. The light source for excitation was a continuous wave 1000 W xenon arc lamp from a Spex Fluorolog-2 spectrofluorometer, equipped with excitation and emission monochromators with dispersion of 4 nm/mm (SPEX, 1681B). The excitation energy was selected by excitation-

fluorescence spectroscopy. To prevent artefacts associated with the presence of linear polarization in the emission,^{S1} a high-quality linear polarizer was placed in the sample compartment, and aligned so that the excitation beam was linearly polarized in the direction of emission detection (z-axis). The key feature of this geometry is that it ensures that the molecules that have been excited and that are subsequently emitting are isotropically distributed in the plane (x,y) perpendicular to the direction of emission detection. The optical system detection consisted of a focusing lens, long pass filter, and 0.22 m monochromator. The emitted light was detected by a cooled EMI-9558B photomultiplier tube operating in photo-counting mode.

S1.5. Electrochemistry

Cyclic voltammograms (Metrohm Autolab) were done using a three-electrode set up with a platinum layer (surface 8 mm x 7.5 mm) as the working electrode, a platinum wire as the counter electrode, and Ag/AgCl as the reference electrode. A 0.1 M solution of tetrabutylammonium hexafluorophosphate (TBAPF₆) in dry acetonitrile was used as the electrolyte solvent in which the compounds were dissolved to achieve a concentration of around 1 mM. All redox potentials were reported *vs.* ferrocene as internal standard. The solutions were purged with argon before the measurements, which were performed under the same inert atmosphere.

S1.6. Quantum mechanical calculations

Quantum mechanical calculations were performed in Gaussian 16, using the “arina” computational resources provided by the UPV-EHU. Ground state energy minimizations were performed using hybrid B3LYP functional, within the Density Functional Theory (DFT), together with the triple valence basis set with a polarization function (6-311g*). The optimized geometries were taken as a true energy minimum using frequency calculations (no negative frequencies). The absorption transition was simulated from the ground state optimized geometry as a Franck-Condon vertical transition using the Time Dependent (TD-DFT) method at the same calculation level and basis set detailed above.

S1.7. Biophotonics

S1.7.1. Fluorescence confocal microscopy

Cell culture: Mouse embryonic fibroblasts (MEFs) were obtained from the American Type Culture Collection (ATCC CRL-2991). MEFs were cultured in Dulbecco modified Eagle medium high glucose (DMEM 25 mM glucose) supplemented with 10% premium fetal bovine serum (FBS, South Africa S1300; Biowest, Nuallé, France), 1% non-essential amino acids (MEM-NEA) and 1% penicillin/streptomycin (final concentration of 100 U/ml penicillin and 100 µg/ml streptomycin), from

Gibco. Cells were grown in a humidified incubator (Thermo Fisher Steri-Cycle Shape with HEPA filter, 5% CO₂) at 37 °C and maintained at 80% confluence in Flask T75 (Nunc). For confocal microscopy imaging, cells were collected and seeded in an 8-chamber LabTek® slide (Thermofisher), and incubated at 37 °C to a final concentration of 10⁵ cells/well. Prior to confocal fluorescence imaging, MEFs were supplemented with **NBDP-4** and LysotrackerTM Red (500 nM and 4 nM final concentration, respectively). Labelled MEFs were then imaged at different incubation times (0 h, 1 h, and 8 h).

Confocal scanning laser microscopy: Fluorescence micrographs by confocal scanning laser microscopy (CSLM) were collected using a Nikon Ti-E inverted microscope equipped with a Nikon C2 confocal scanning confocal module, 488-nm and 561-nm continuous lasers, emission band-pass filters (525/ 50 and dichroic 561LP for the green and red channel, respectively) and a Nikon Plan Apo λ 100 \times 1.45 oil ∞ /0.17 WD 0.13 immersion objective (Nikon ref. CFI Plan Apo DM Lambda 100X Oil). Co-localization analysis was performed on whole images and the Pearson's coefficient, R, was calculated with the JaCoP plug-in for Image J.^{S2}

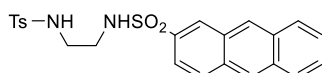
S2. Synthetic procedures and characterization data

S2.1. Synthesis of bis(sulfonamide)s

N-(2-aminoethyl)-4-methylbenzene-1-sulfonamide was obtained from ethane-1,2-diamine and tosyl chloride in an optimized 86% yield, following the described synthetic procedure.^{S4}

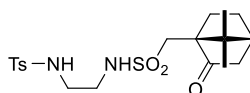
N-(2-aminoethyl)butane-1-sulfonamide was obtained from ethane-1,2-diamine and butane-1-sulfonyl chloride in an optimized 92% yield, following the described synthetic procedure.^{S4}

Synthesis of I-1:



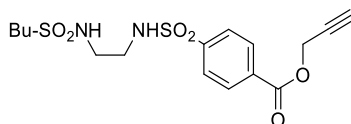
Anthracene-2-sulfonyl chloride (102 mg, 0.37 mmol) was portionwise added over a stirred solution to *N*-(2-aminoethyl)-4-methylbenzene-1-sulfonamide (79 mg, 0.37 mmol) and triethylamine (37 mg, 0.37 mmol) in CH₂Cl₂ (10 mL) at 0 °C. The resulting mixture was stirred at room temperature for 24 h. Then, CH₂Cl₂ (15 mL) and H₂O (15 mL) were added, the two layers were separated and the aqueous layer was extracted with CH₂Cl₂ (3 × 15 mL). The combined organic layers were washed with brine (1 × 15 mL) and dried over anhydrous Na₂SO₄. After filtration and solvent evaporation under reduced pressure, the residue was purified by recrystallization (petroleum ether/AcOEt) to obtain **I-1** (126 mg, 75%) as a white solid. ¹H NMR (DMSO-*d*₆, 300 MHz) δ 8.87 (s, 1H), 8.72 (s, 1H), 8.55 (s, 1H), 8.27 (d, *J* = 9.1 Hz, 1H), 8.18 (m, 2H), 7.87 (t, *J* = 5.8 Hz, 1H), 7.71-7.60 (m, 3H), 7.59 (t, *J* = 6.0 Hz, 1H), 7.49 (d, *J* = 8.3 Hz, 2H), 7.17 (d, *J* = 8.0 Hz, 2H), 2.87-2.77 (m, 2H), 2.75-2.65 (m, 2H), 2.20 (s, 3H) ppm.

Synthesis of I-2:



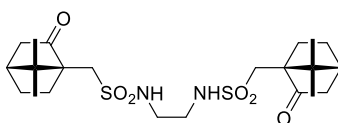
Following a similar procedure to that used for **I-1**, *N*-(2-aminoethyl)-4-methylbenzene-1-sulfonamide (500 mg, 2.33 mmol) was reacted with (1*S*)-camphor-10-sulfonyl chloride (585 mg, 2.33 mmol). The reaction crude was purified by flash chromatography (silica gel, CH₂Cl₂/MeOH 99:1) to obtain **I-2** (910 mg, 91%) as a white solid. [α]_D²⁰ +13.2 (*c* 5.00, CHCl₃). ¹H NMR (CDCl₃, 300 MHz) δ 7.74 (d, *J* = 8.3 Hz, 2H), 7.30 (d, *J* = 7.9 Hz, 2H), 5.64 (t, *J* = 6.1 Hz, 1H), 5.38 (t, *J* = 6.2 Hz, 1H), 3.42 (d, *J* = 15.1 Hz, 1H), 3.37-3.21 (m, 2H), 3.16-3.07 (m, 2H), 2.93 (d, *J* = 15.1 Hz, 1H), 2.39 (ddd, *J* = 18.6, 4.9, 3.0 Hz, 1H), 2.41 (s, 3H), 2.23 (ddd, *J* = 14.1, 10.8, 3.6 Hz, 1H), 2.12 (t, *J* = 4.4 Hz, 1H), 2.09-1.98 (m, 1H), 1.96 (d, *J* = 18.6 Hz, 1H), 1.95-1.84 (m, 1H), 1.46 (ddd, *J* = 12.4, 8.9, 3.5 Hz, 1H), 1.01 (s, 3H), 0.89 (s, 3H) ppm. ¹³C NMR (CDCl₃, 75 MHz) δ 217.6 (C), 143.7 (C), 136.7 (C), 129.9 (CH), 127.2 (CH), 59.2 (C), 49.9 (CH₂), 49.1 (C), 43.5 (CH₂), 43.4 (CH₂), 43.1 (CH₂), 42.9 (CH), 27.1 (CH₂), 26.4 (CH₂), 21.7 (CH₃), 20.0 (CH₃), 19.6 (CH₃) ppm. FTIR ν 3289, 1742, 1332, 1140 cm⁻¹.

Synthesis of I-3:



I-3 was obtained from *N*-(2-aminoethyl)butane-1-sulfonamide in three steps in 87% overall yield, as described by us.^{S3} Copy of NMR spectra, which were missing in preliminary ref. S3, have been included in this publication (section S3).

Synthesis of I-4:

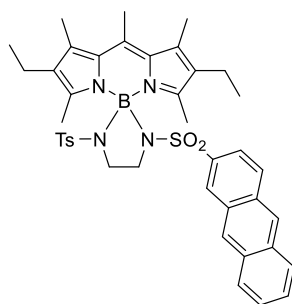


(Intermediate bis(sulfonamide) based on camphor for the synthesis of **NBDP-9**)

A solution of NaOH (82 mg, 2.05 mmol) and ethane-1,2-diamine (62 mg, 1.02 mmol) in distilled water (10 mL) was added over a solution of (1*S*)-camphor-10-sulfonyl chloride (514 mg, 2.05 mmol) in diethyl ether (10 mL) at 0 °C. The cooling bath was removed, and the reaction mixture was vigorously stirred at room temperature for 24 h. Then, CH₂Cl₂ (15 mL) and H₂O (15 mL) were added, the two layers were separated and the aqueous layer was extracted with CH₂Cl₂ (3 × 15 mL). The combined organic layers were washed with brine (1 × 15 mL) and dried over anhydrous Na₂SO₄. After filtration and solvent evaporation under reduced pressure, the residue was purified by flash column chromatography (silica gel, hexane/AcOEt 7:3) to obtain **I-4** (452 mg, 90%) as a white solid. $[\alpha]_D^{20} +29.1$ (*c* 5.00, CHCl₃). ¹H NMR (CDCl₃, 300 MHz) δ 5.65 (br s, 2H), 3.45 (d, *J* = 15.6 Hz, 2H), 3.40 (t, *J* = 2.8 Hz, 4H), 2.94 (d, *J* = 15.1 Hz, 2H), 2.39 (ddd, *J* = 18.7, 4.9, 3.0 Hz, 2H), 2.25 (ddd, *J* = 14.1, 10.7, 3.6 Hz, 2H), 2.12 (t, *J* = 4.4 Hz, 2H), 2.03 (m, 2H), 1.93 (d, *J* = 18.6 Hz, 2H), 1.94-1.85 (m, 2H), 1.45 (ddd, *J* = 12.3, 8.7, 3.7 Hz, 2H), 1.02 (s, 6H), 0.90 (s, 6H) ppm. ¹³C NMR (CDCl₃, 75 MHz) δ 216.9 (C), 59.0 (C), 49.6 (CH₂), 48.9 (CH₂), 43.8 (C), 42.9 (CH₂), 42.8 (CH), 27.1 (CH₂), 26.0 (CH₂), 19.9 (CH₃), 19.6 (CH₃) ppm. FTIR ν 3292, 1740, 1327, 1146 cm⁻¹.

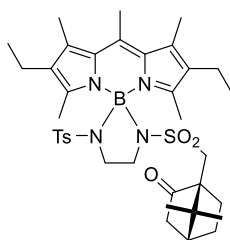
S2.2. Synthesis of *N*-BODIPYs

Synthesis of NBDP-5:



Under argon atmosphere, 1 M BCl_3 solution (CH_2Cl_2 , 0.32 mL, 0.32 mmol) was dropwise added over a solution of commercial 2,6-diethyl-1,3,5,7,8-pentamethyl-*F*-BODIPY (PM567, **FBDP-1**; 50 mg, 0.16 mmol) in dry CH_2Cl_2 (5 mL). The reaction mixture was stirred for 5 min (disappearance of starting BODIPY was monitored by TLC). Then, triethylamine (130 mg, 1.28 mmol) was added, followed by **I-1** (214 mg, 0.48 mmol), and the mixture stirred for 30 min (the reaction progress was monitored by TLC). Then, the reaction mixture was filtered through Celite® S, and washed with CH_2Cl_2 and the solvent was evaporated under reduced pressure. The reaction crude was purified by flash chromatography (silica gel, hexane/AcOEt 7:3) to obtain **NBDP-5** (40 mg, 35%) as a reddish orange solid. $R_F = 0.20$ (hexano/EtOAc 6:4). ^1H NMR (CDCl_3 , 300 MHz) δ 8.39 (s, 1H), 8.33 (s, 1H), 8.07 (sa, 1H), 8.02 (m, 2H), 7.82 (d, $J = 8.9$ Hz, 1H), 7.54 (m, 2H), 7.21 (dd, $J = 8.8, 1.8$ Hz, 1H), 7.20 (d, $J = 8.2$ Hz, 2H), 7.04 (d, $J = 8.0$ Hz, 2H), 3.75-3.65 (m, 2H), 3.62-3.52 (m, 2H), 2.68 (s, 3H), 2.41 (s, 6H), 2.33 (s, 3H), 2.21 y 2.13 (ABX₃ system, AB part, $J_{AB} = 14.5$ Hz, $J_{AX} = J_{BX} = 7.5$ Hz, 4H), 1.73 (s, 6H), 0.96 (ABX₃ system, X part, $J_{AX} = J_{BX} = 7.5$ Hz, 6H) ppm. ^{13}C NMR (CDCl_3 , 75 MHz) δ 151.6 (C), 142.1 (C), 140.1 (C), 137.3 (C), 136.7 (C), 136.4 (C), 133.2 (C), 133.1 (C), 132.8 (C), 132.2 (C), 131.6 (C), 129.8 (C), 129.1 (CH), 128.9 (CH), 128.7 (CH), 128.4 (CH), 128.3 (CH), 126.9 (CH), 126.8 (CH), 126.4 (CH), 121.9 (CH), 44.7 (CH₂), 44.4 (CH₂), 21.5 (CH₃), 17.8 (CH₃), 17.4 (CH₂), 15.16 (CH₃), 15.09 (CH₃), 12.3 (CH₃) ppm. ^{11}B NMR (CDCl_3 , 160 MHz) δ -0.94 (s) ppm. FTIR ν 1526, 1479, 1326, 1192 cm^{-1} . HRMS (ESI) m/z : $[\text{M} + \text{H}]^+$ Calcd. for $\text{C}_{41}\text{H}_{46}\text{BN}_4\text{O}_4\text{S}_2$ 733.3048; Found 733.3046.

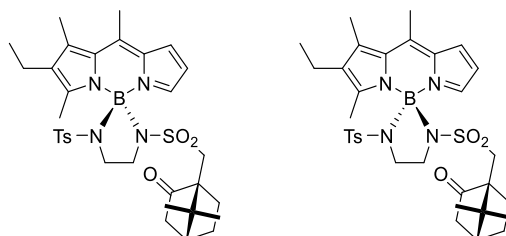
Synthesis of NBDP-6:



Following a similar procedure to that used for **NBDP-5**, **FBDP-1** (50 mg, 0.16 mmol) was reacted with **I-2** (206 mg, 0.48 mmol). The reaction crude was purified flash chromatography (silica gel, hexane/AcOEt 6:4) to obtain **NBDP-6** (87 mg, 78%) as an orange solid. $R_F = 0.15$ (hexane/ AcOEt 6:4).

$[\alpha]_D^{20}$ -56.1 (c 0.112, CHCl_3). $^1\text{H NMR}$ (CDCl_3 , 300 MHz) δ 7.27 (d, J = 8.1 Hz, 2H), 7.10 (d, J = 8.0 Hz, 2H), 3.83-3.58 (m, 4H), 3.15 (d, J = 14.2 Hz, 1H), 2.68 (s, 3H), 2.39 (s, 3H), 2.37 (s, 3H), 2.366 (s, 3H), 2.42-2.30 (m, 5H), 2.25 (dm, J = 18.5 Hz, 1H), 2.13 (s, 3H), 2.06 (d, J = 14.2 Hz, 1H), 2.13 (s, 3H), 1.95 (t, J = 4.5 Hz, 1H), 1.92-1.76 (m, 1H), 1.82 (d, J = 18.4 Hz, 1H), 1.43 (m, 1H), 1.26 (m, 1H), 1.03 (t, J = 7.2 Hz, 3H), 1.00 (t, J = 7.2 Hz, 3H), 0.84 (s, 3H), 0.59 (s, 3H) ppm. $^{13}\text{C NMR}$ (CDCl_3 , 75 MHz) δ 215.4 (C), 152.8 (C), 149.4 (C), 142.2 (C), 140.2 (C), 137.6 (C), 137.4 (C), 136.0 (C), 133.7 (C), 133.5 (C), 133.0 (C), 132.4 (C), 129.2 (CH), 127.0 (CH), 58.1 (C), 47.6 (C), 46.1 (CH_2), 45.4 (CH_2), 44.2 (CH_2), 42.7 (CH_2), 42.5 (CH), 27.0 (CH_2), 24.6 (CH_2), 21.6 (CH_3), 20.0 (CH_3), 19.6 (CH_3), 17.8 (CH_3), 17.5 (CH_2), 17.5 (CH_2), 15.3 (CH_3), 15.2 (CH_3), 15.0 (CH_3), 14.96 (CH_3), 12.8 (CH_3), 12.7 (CH_3) ppm. $^{11}\text{B NMR}$ (CDCl_3 , 160 MHz) δ -1.04 (s) ppm. FTIR ν 1744, 1563, 1480, 1329, 1193, 1052, 980 cm^{-1} . HRMS (ESI) m/z : $[\text{M} + \text{Na}]^+$ Calcd. for $\text{C}_{37}\text{H}_{51}\text{BN}_4\text{O}_5\text{S}_2\text{Na}$ 729.3286; Found 729.3298.

Synthesis of NBDP-7-R and NBDP-7-S:

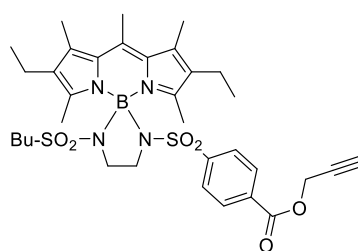


Following a similar procedure to that used for **NBDP-5**, 2-ethyl-1,3,8-trimethyl-*F*-BODIPY (**FBDP-2**)^{S5} (50 mg, 0.19 mmol) was reacted with **I-2** (254 mg, 0.57 mmol). The reaction crude containing both diastereomers was purified by flash chromatography (silica gel, pentane/diethyl ether/AcOEt 5:4:1) to obtain, first, **NBDP-7-S** and then, **NBDP-7-R**. The absolute configuration was determined by X-Ray diffraction (see Table S3 and Figure S4).

NBDP-7-S: 49 mg (39%). Orange solid. R_F = 0.09 (pentane/diethyl ether/AcOEt 5:4:1). $[\alpha]_D^{20}$ -323 (c 0.072, CHCl_3). $^1\text{H NMR}$ (CDCl_3 , 300 MHz) δ 7.22 (d, J = 8.2 Hz, 2H), 7.09 (d, J = 8.0 Hz, 2H), 7.03 (d, J = 3.6 Hz, 1H), 6.86 (br s, 1H), 6.24 (dd, J = 4.0, 2.2 Hz, 1H), 3.78-3.65 (m, 3H), 3.62-3.50 (m, 1H), 2.73 (d, J = 14.4 Hz, 1H), 2.65 (s, 3H), 2.44 (d, J = 14.4 Hz, 2H), 2.41 (s, 3H), 2.39 (s, 3H), 2.37 (s, 3H), 2.27-2.18 (m, 2H), 1.94 (t, J = 4.5 Hz, 1H), 1.90-1.81 (m, 1H), 1.76 (d, J = 18.3 Hz, 1H), 1.25-1.12 (m, 2H), 1.06 (t, J = 7.6 Hz, 3H), 0.93 (s, 3H), 0.69 (s, 3H) ppm. $^{13}\text{C NMR}$ (CDCl_3 , 75 MHz) δ 215.4 (C), 161.2 (C), 142.2 (C), 142.0 (C), 140.4 (C), 137.5 (C), 136.6 (CH), 135.8 (C), 134.9 (C), 129.2 (CH), 127.0 (CH), 122.0 (CH), 114.9 (CH), 58.3 (C), 47.7 (C), 47.1 (CH_2), 45.1 (CH_2), 44.5 (CH_2), 42.8 (CH), 42.7 (CH_2), 27.0 (CH_2), 24.6 (CH_2), 21.6 (CH_3), 20.1 (CH_3), 19.8 (CH_3), 17.4 (CH_2), 17.2 (CH_3), 15.02 (CH_3), 14.98 (CH_3), 14.1 (CH_3) ppm. $^{11}\text{B NMR}$ (CDCl_3 , 160 MHz) δ -1.35 (s) ppm. FTIR ν 1743, 1575, 1328, 1174 cm^{-1} . HRMS (ESI) m/z : $[\text{M} + \text{Na}]^+$ Calcd. for $\text{C}_{33}\text{H}_{43}\text{BN}_4\text{O}_5\text{S}_2\text{Na}$ 673.2660; Found 673.2661.

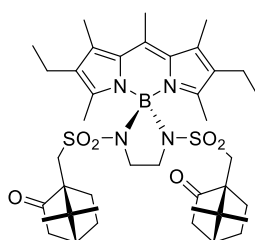
NBDP-7-R: 46 mg (37%). Orange solid. $R_F = 0.08$ (pentane/diethyl ether/AcOEt 5:4:1). $[\alpha]_D^{20} +278$ (c 0.102, CHCl_3). $^1\text{H NMR}$ (CDCl_3 , 300 MHz) δ 7.26 (d, $J = 8.1$ Hz, 2H), 7.11 (d, $J = 8.0$ Hz, 2H), 7.01 (d, $J = 3.5$ Hz, 1H), 6.94 (br s, 1H), 6.28 (dd, $J = 3.9, 2.3$ Hz, 1H), 3.82-3.55 (m, 4H), 3.19 (d, $J = 14.3$ Hz, 1H), 2.64 (s, 3H), 2.42 (q, $J = 7.6$ Hz, 2H), 2.41 (s, 3H), 2.38 (s, 3H), 2.37 (s, 3H), 2.34 (m, 1H), 2.25 (dm, $J = 18.0$ Hz, 1H), 1.95 (t, $J = 4.5$ Hz, 1H), 1.92-1.88 (m, 1H), 1.83 (d, $J = 18.4$ Hz, 1H), 1.73 (d, $J = 14.3$ Hz, 1H), 1.57-1.44 (m, 2H), 1.33-1.23 (m, 2H), 1.08 (t, $J = 7.6$ Hz, 3H), 0.75 (s, 3H), 0.55 (s, 3H) ppm. $^{13}\text{C NMR}$ (CDCl_3 , 75 MHz) δ 215.4 (C), 162.8 (C), 142.4 (C), 142.3 (C), 139.5 (C), 137.6 (C), 136.3 (C), 136.2 (C), 135.6 (CH), 134.7 (C), 129.3 (CH), 126.9 (CH), 121.1 (CH), 114.5 (CH), 57.9 (C), 47.9 (C), 45.9 (CH_2), 45.0 (CH_2), 44.4 (CH_2), 42.7 (CH_2), 42.3 (CH), 27.1 (CH_2), 24.5 (CH_2), 21.6 (CH_3), 19.7 (CH_3), 19.6 (CH_3), 17.4 (CH_2), 16.9 (CH_3), 14.9 (CH_3), 14.7 (CH_3), 14.1 (CH_3) ppm. $^{11}\text{B NMR}$ (CDCl_3 , 160 MHz) δ -1.35 (s) ppm. FTIR ν 1744, 1578, 1399, 1176 cm^{-1} . HRMS (ESI) m/z : $[\text{M} + \text{H}]^+$ Calcd. for $\text{C}_{33}\text{H}_{44}\text{BN}_4\text{O}_5\text{S}_2$ 651.2841; Found 651.2841.

Synthesis of NBDP-8:



NBDP-8 was synthesized from **FBDP-1** and **I-3**, as described by us.^{S3} Copy of NMR spectra, as well as HRMS, which were missing in preliminary ref. S3, have been included in this publication (section S3). HRMS (ESI) m/z : $[\text{M} + \text{H}]^+$ Calcd. for $\text{C}_{34}\text{H}_{46}\text{BN}_4\text{O}_6\text{S}_2$ 681.2946; Found 681.2953.

Synthesis of NBDP-9:

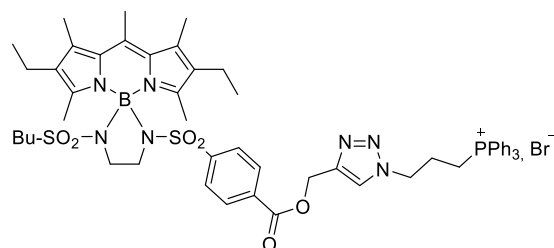


Following a similar procedure to that used for **NBDP-5**, **FBDP-1** (50 mg, 0.16 mmol) was reacted with **I-4** (230 mg, 0.48 mmol). The reaction crude was purified flash chromatography (silica gel, hexane/AcOEt 7:3) to obtain **NBDP-9** (110 mg, 92%) as an orange solid. $R_F = 0.10$ (hexane/ AcOEt 6:4). $[\alpha]_D^{20} +104$ (c 0.11, CHCl_3). $[\alpha]_D^{20} 125$ (c 0.01 CHCl_3). $^1\text{H NMR}$ (CDCl_3 , 300 MHz) δ 3.86 (m, 4H), 3.27 (d, $J = 14.2$ Hz, 2H), 2.63 (s, 3H), 2.47 (s, 6H), 2.45-2.36 (m, 6H), 2.33 (s, 6H), 2.26 (md, $J = 18.5$ Hz, 2H), 2.11 (d, $J = 14.2$ Hz, 2H), 1.96 (t, $J = 4.5$ Hz, 2H), 1.88 (m, 2H), 1.84 (d, $J = 18.4$ Hz, 2H), 1.48 (ddd, $J = 14.0, 9.4, 4.6$ Hz, 2H), 1.28 (ddd, $J = 12.4, 9.0, 3.5$ Hz, 2H), 1.00 (t, $J = 7.5$ Hz, 6H),

0.86 (s, 6H), 0.62 (s, 6H) ppm. ^{13}C NMR (CDCl_3 , 75 MHz) δ 215.4 (C), 150.5 (C), 140.5 (C), 137.0 (C), 133.5 (C), 133.2 (C), 58.1 (C), 47.6 (C), 46.3 (CH_2), 45.1 (CH_2), 42.7 (CH_2), 42.5 (CH), 27.0 (CH_2), 24.6 (CH_2), 20.0 (CH_3), 19.6 (CH_3), 17.7 (CH_3), 17.5 (CH_2), 15.2 (CH_3), 15.0 (CH_3), 13.3 (CH_3) ppm. ^{11}B NMR (CDCl_3 , 160 MHz) δ -1.06 (s) ppm. FTIR ν 1744, 1563, 1480, 1324, 1193, 1048, 979 cm^{-1} . HRMS (ESI) m/z : $[\text{M} + \text{H}]^+$ Calcd. for $\text{C}_{40}\text{H}_{60}\text{BN}_4\text{O}_6\text{S}_2$; 767.4042; Found 767.4053.

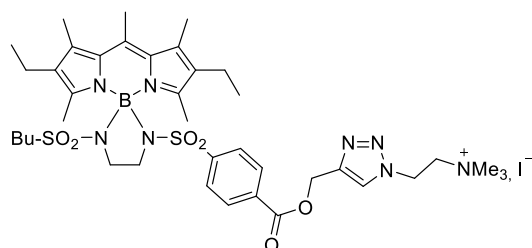
S2.3. Synthesis of bioprobes by click chemistry

Synthesis of NBDP-2:



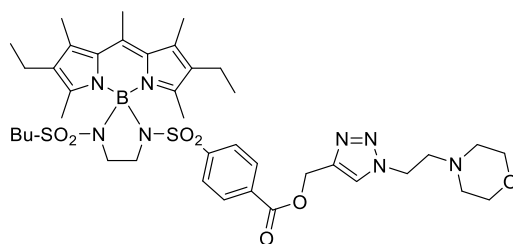
NBDP-2 was synthesized from **NBDP-8** following the procedure described by us.^{S3} See spectral characterization in ref. S3. Copy of NMR spectra, as well as HRMS, which were not in preliminary ref. S3, have been included in this publication (section S3). HRMS (ESI) m/z : $[\text{M}]^+$ Calcd. for $\text{C}_{55}\text{H}_{66}\text{BN}_7\text{O}_6\text{PS}_2$ 1026.4341; Found 1026.4369.

Synthesis of NBDP-3:



NBDP-3 was synthesized from **NBDP-8** following the procedure described by us.^{S3} Copy of NMR spectra, as well as HRMS, which were not in preliminary ref. S3, have been included in this publication (section S3). HRMS (ESI) m/z : $[\text{M}]^+$ Calcd. for $\text{C}_{40}\text{H}_{60}\text{BN}_8\text{O}_6\text{S}_2$ 823.4165; Found 823.4171.

Synthesis of NBDP-4:

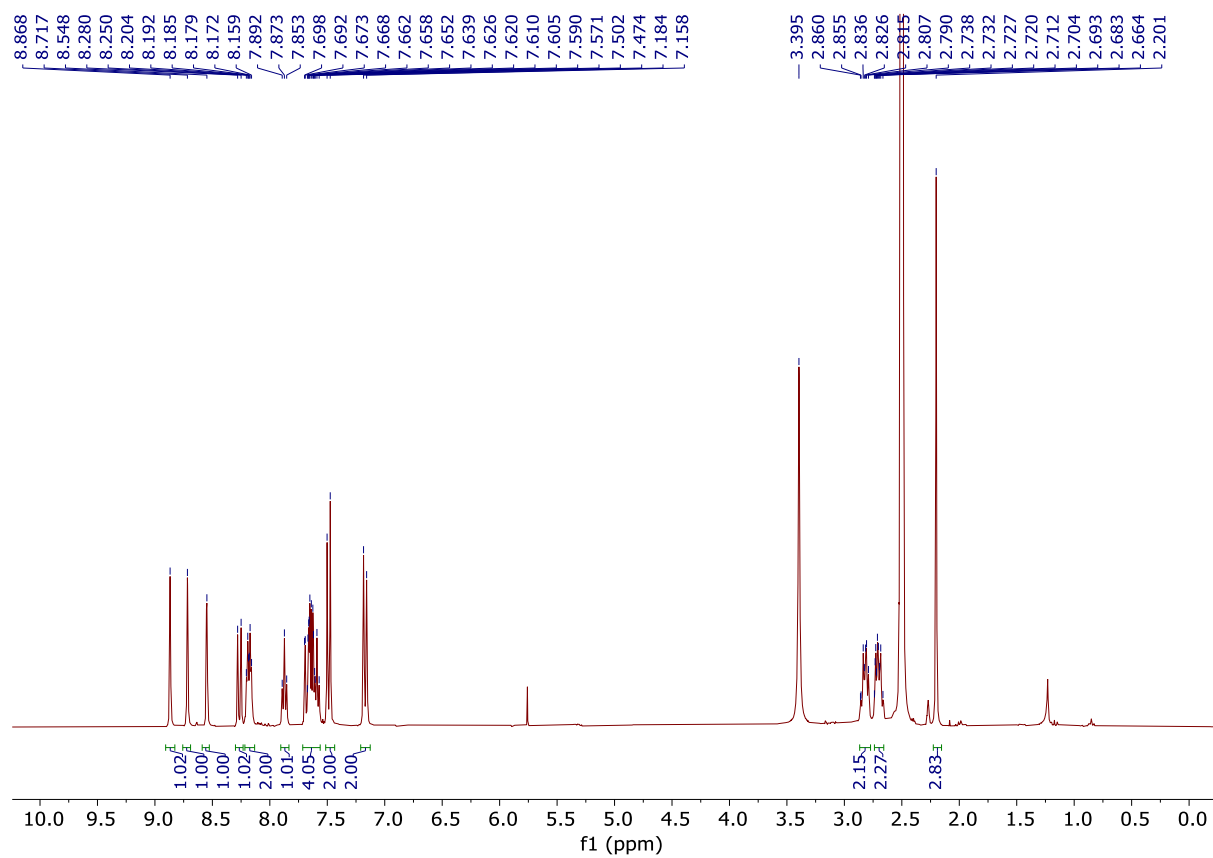


Over a mixture of **NBDP-8** (25 mg, 0.037 mmol) and 4-(2-azidoethyl)morpholine (7 mg, 0.044 mmol) in 2 mL of *t*-butanol, under argon atmosphere, a solution of $\text{CuSO}_4 \cdot 5\text{H}_2\text{O}$ (4 mg, 0.015 mmol) in water

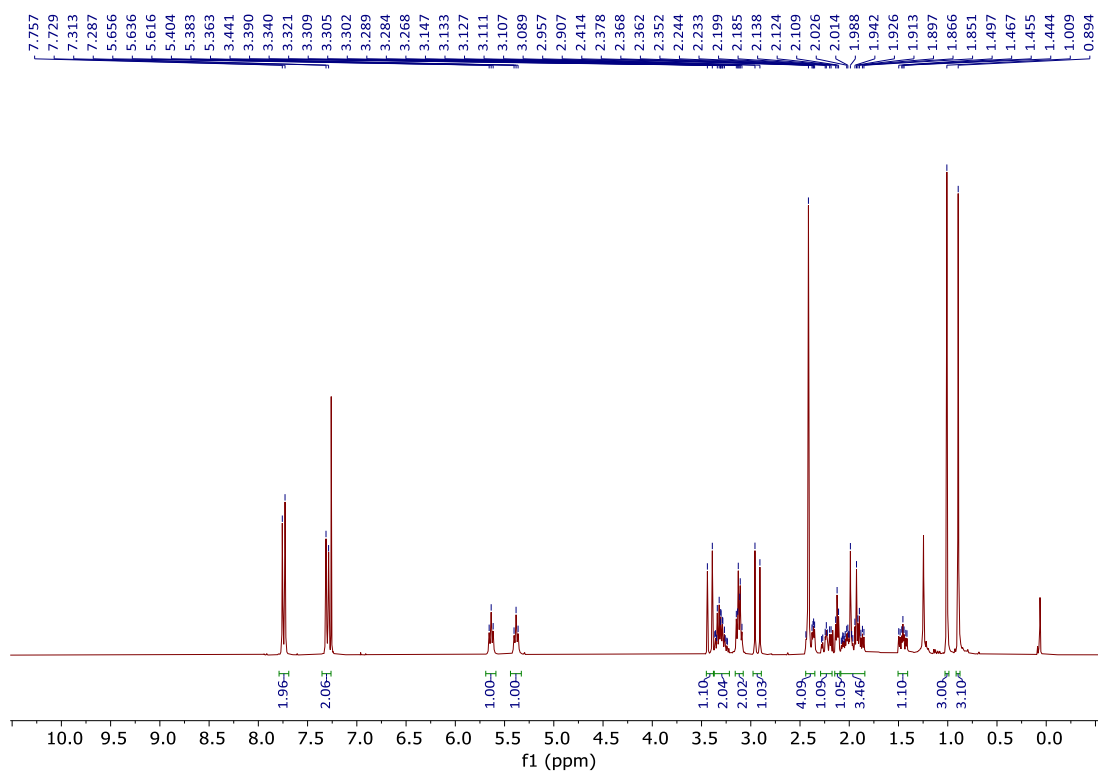
(1 mL) and, immediately, a solution of sodium ascorbate (6 mg, 0.030 mmol) in water (1 mL) were added dropwise. The reaction mixture was stirred at room temperature for 24 h (disappearance of **NBDP-8** was monitored by TLC). Then, CH₂Cl₂ (15 mL) and H₂O (15 mL) were added, the two layers were separated and the aqueous layer was extracted with CH₂Cl₂ (3 × 15 mL). The combined organic layers were washed with brine (1 × 15 mL) and dried over anhydrous Na₂SO₄. After filtration and solvent evaporation under reduced pressure the obtained residue was purified by flash chromatography (silica gel, CH₂Cl₂/MeOH 95:5) to obtain **NBDP-4** (26 mg, 85%) as a red solid. *R*_F = 0.34 (CH₂Cl₂/MeOH 95:5). ¹H NMR (CDCl₃, 300 MHz) δ 7.94 (d, *J* = 8.3 Hz, 2H), 7.83 (s, 1H), 7.38 (d, *J* = 8.4 Hz, 2H), 5.49 (s, 2H), 4.48 (t, *J* = 6.3 Hz, 2H), 3.73-3.60 (m, 8H), 2.83 (t, *J* = 6.3 Hz, 2H), 2.69 (s, 3H), 2.53-2.42 (m, 6H), 2.46-2.23 (m, 4H), 2.38 (s, 6H), 2.04 (s, 6H), 1.54 (m, 2H), 1.22 (sext, *J* = 7.3 Hz, 2H), 0.98 (t, *J* = 7.6 Hz, 6H), 0.78 (t, *J* = 7.3 Hz, 3H) ppm. ¹³C NMR (CDCl₃, 75 MHz) δ 165.4 (C), 150.9 (C), 144.2 (C), 142.4 (C), 140.4 (C), 137.1 (C), 133.3 (C), 133.1 (C), 132.5 (C), 130.0 (CH), 127.0 (CH), 124.9 (CH), 67.0 (CH₂), 58.6 (CH₂), 57.9 (CH₂), 53.6 (CH₂), 51.1 (CH₂), 47.6 (CH₂), 45.1 (CH₂), 44.5 (CH₂), 24.6 (CH₂), 21.9 (CH₂), 17.9 (CH₃), 17.3 (CH₂), 15.1 (2 × CH₃), 13.6 (CH₃), 12.7 (CH₃) ppm. ¹¹B NMR (CDCl₃, 160 MHz) δ -1.08 (s) ppm. FTIR ν 1723, 1562, 1480, 1327, 1193 cm⁻¹. HRMS (ESI) *m/z*: [M + H]⁺ Calcd. for C₄₀H₅₈BN₈O₇S₂ 837.3957; Found 837.3961.

S3. NMR spectra

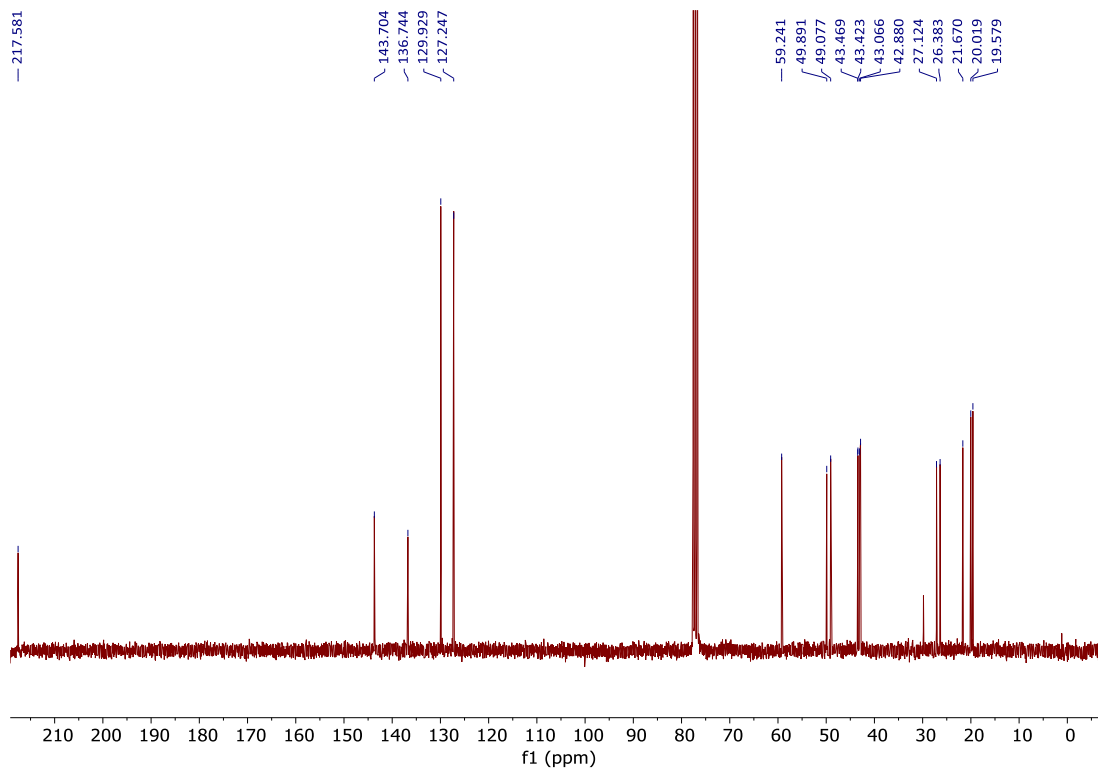
¹H NMR of I-1 (300 MHz, DMSO-d₆)



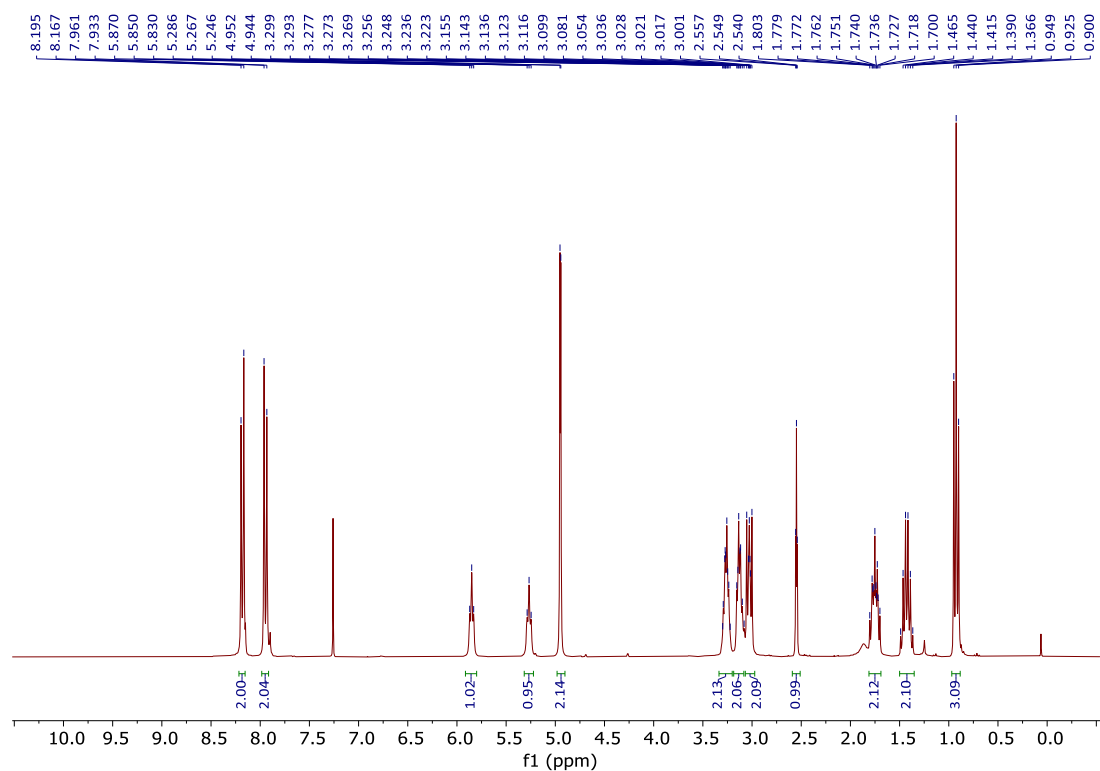
¹H NMR of I-2 (300 MHz, CDCl₃)



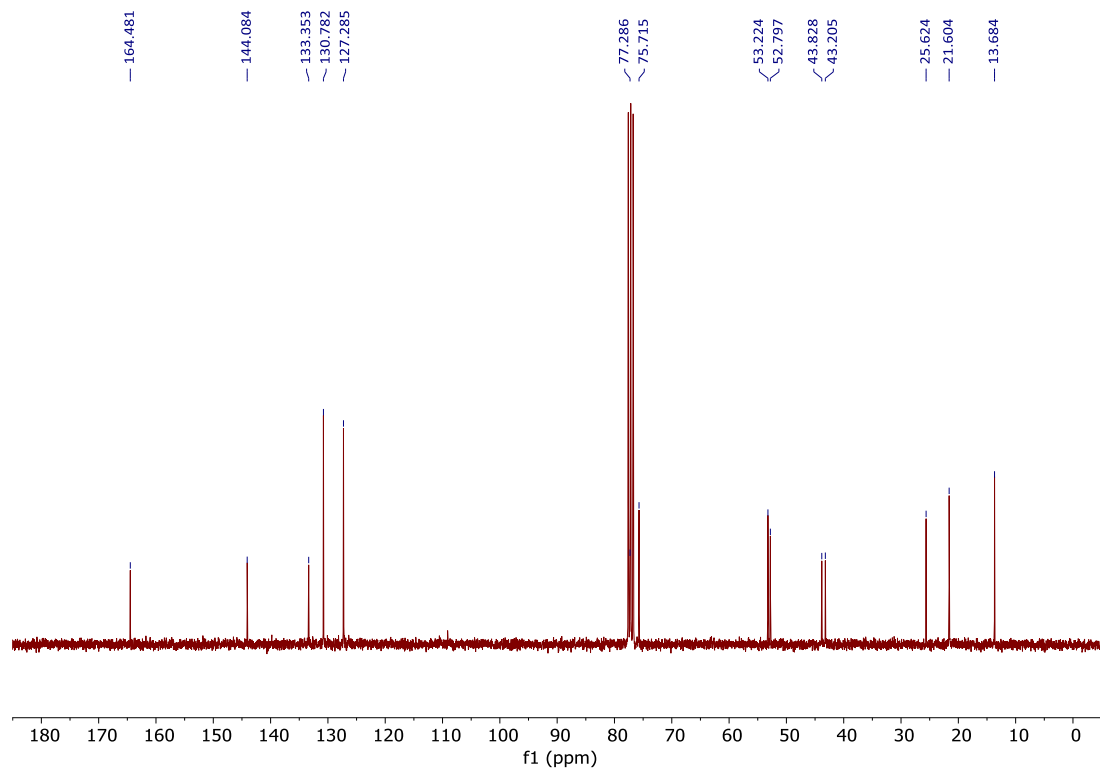
¹³C NMR of I-2 (75 MHz, CDCl₃)



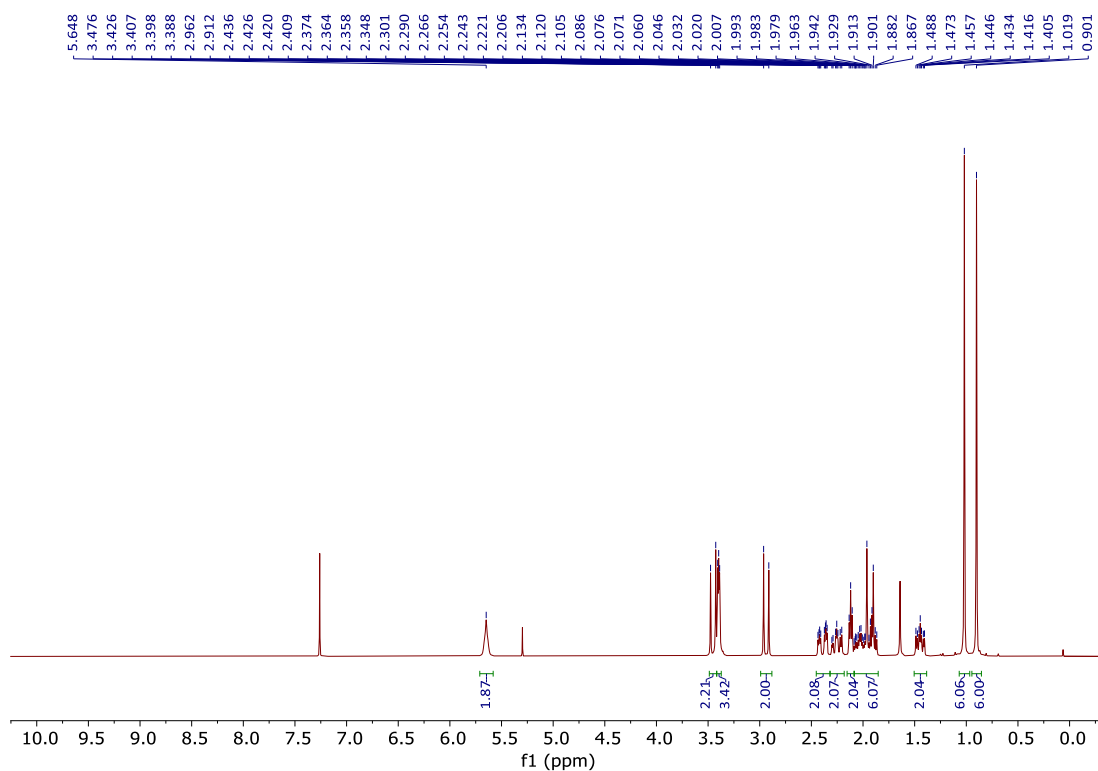
¹H NMR of I-3 (300 MHz, CDCl₃)



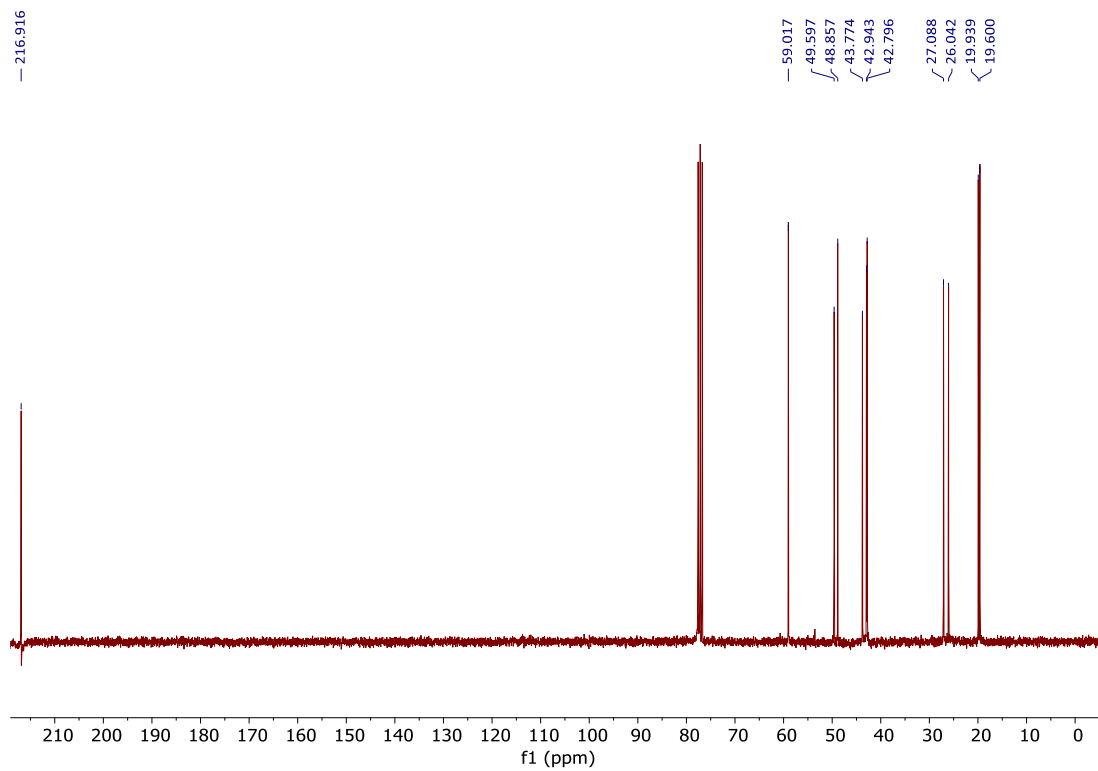
¹³C NMR of I-3 (75 MHz, CDCl₃)



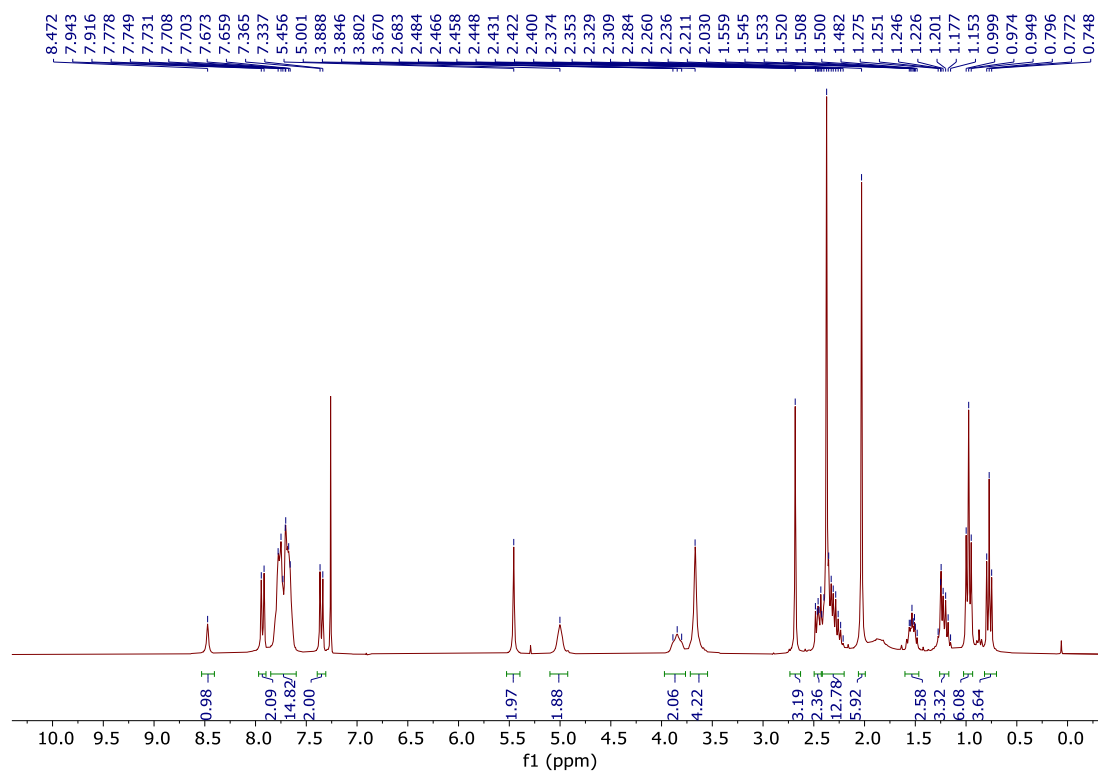
¹H NMR of I-4 (300 MHz, CDCl₃)



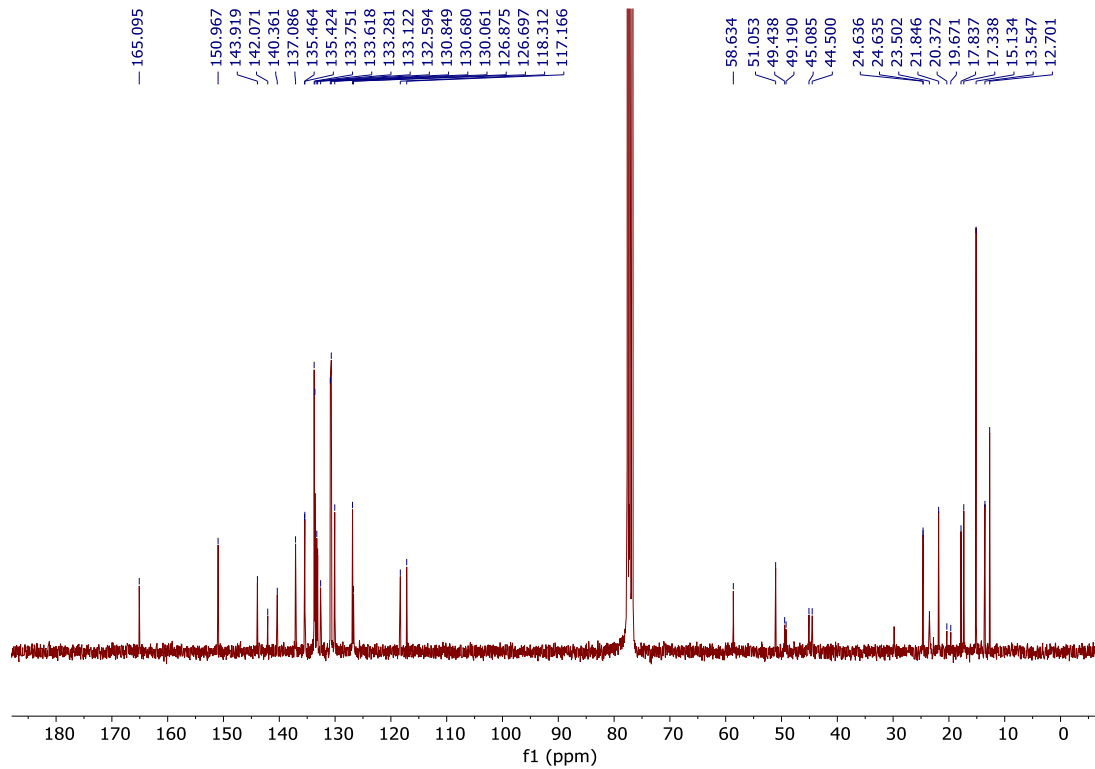
¹³C NMR of I-4 (75 MHz, CDCl₃)



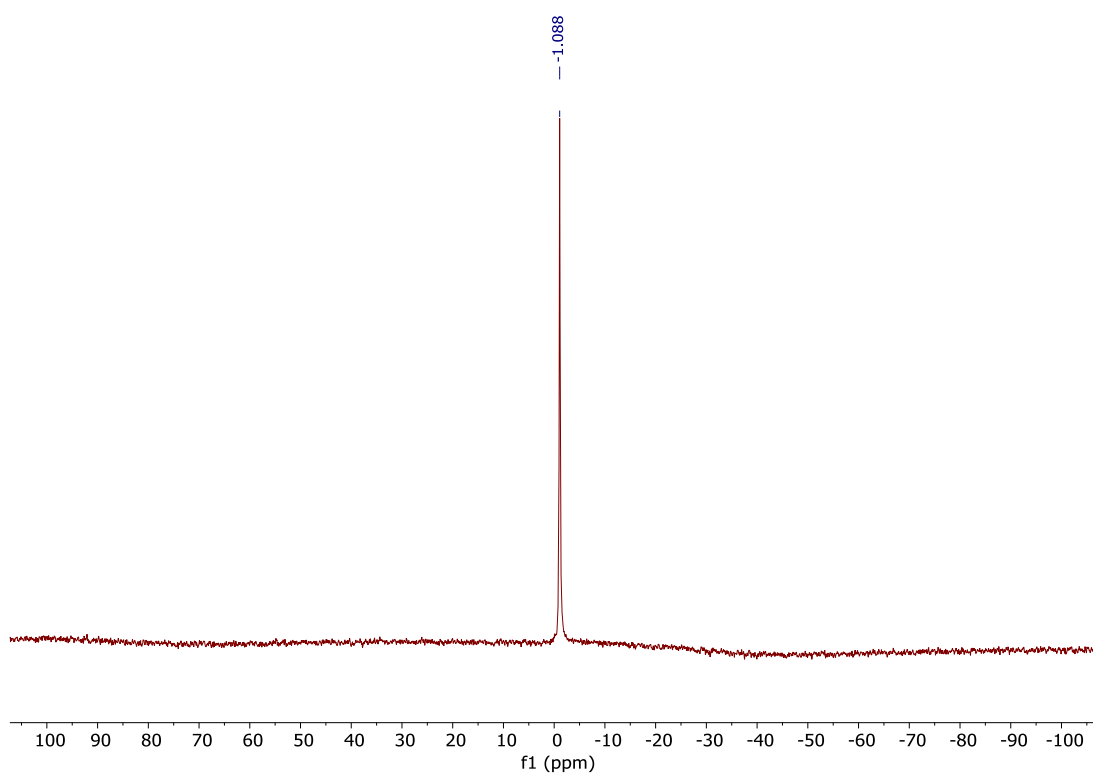
¹H NMR of NBDP-2 (300 MHz, CDCl₃):



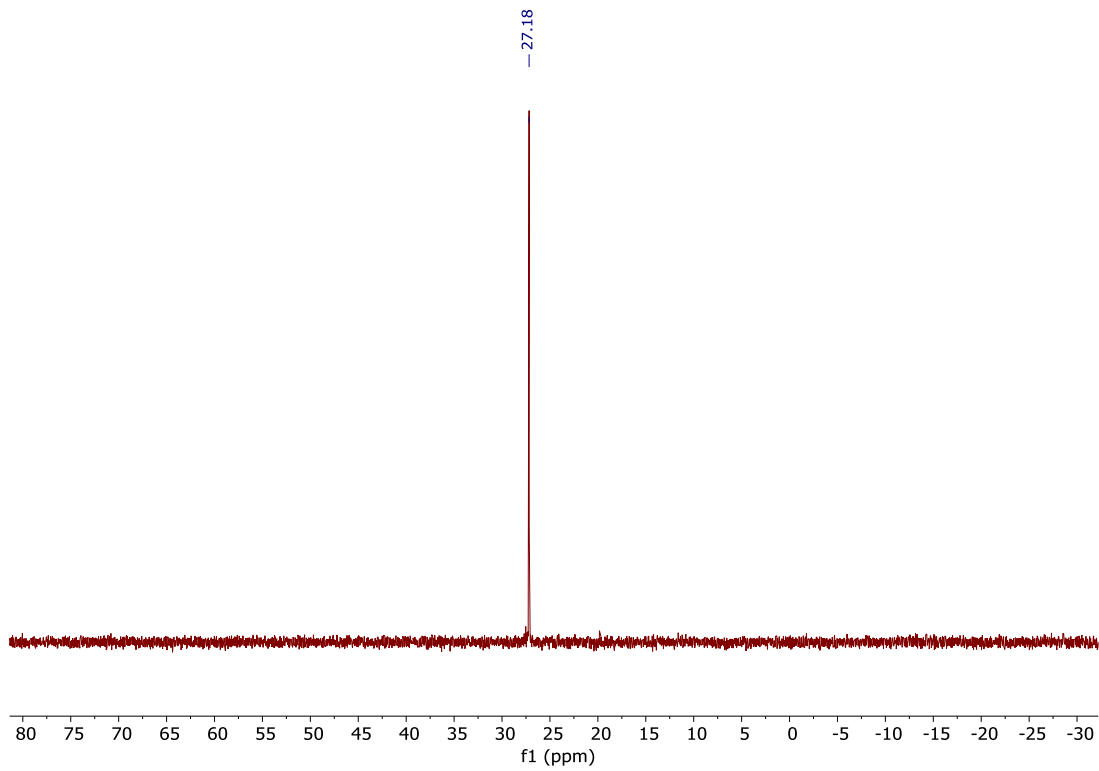
¹³C NMR of NBDP-2 (75 MHz, CDCl₃):



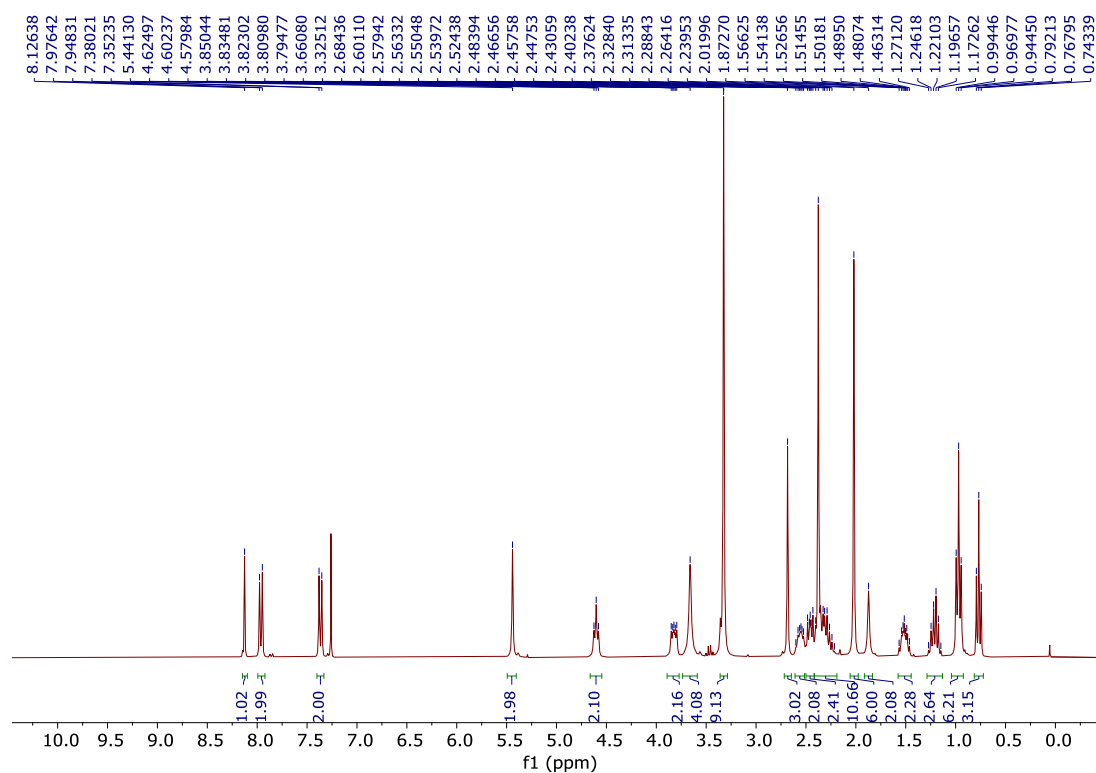
^{11}B NMR of NBDP-2 (160 MHz, CDCl_3):



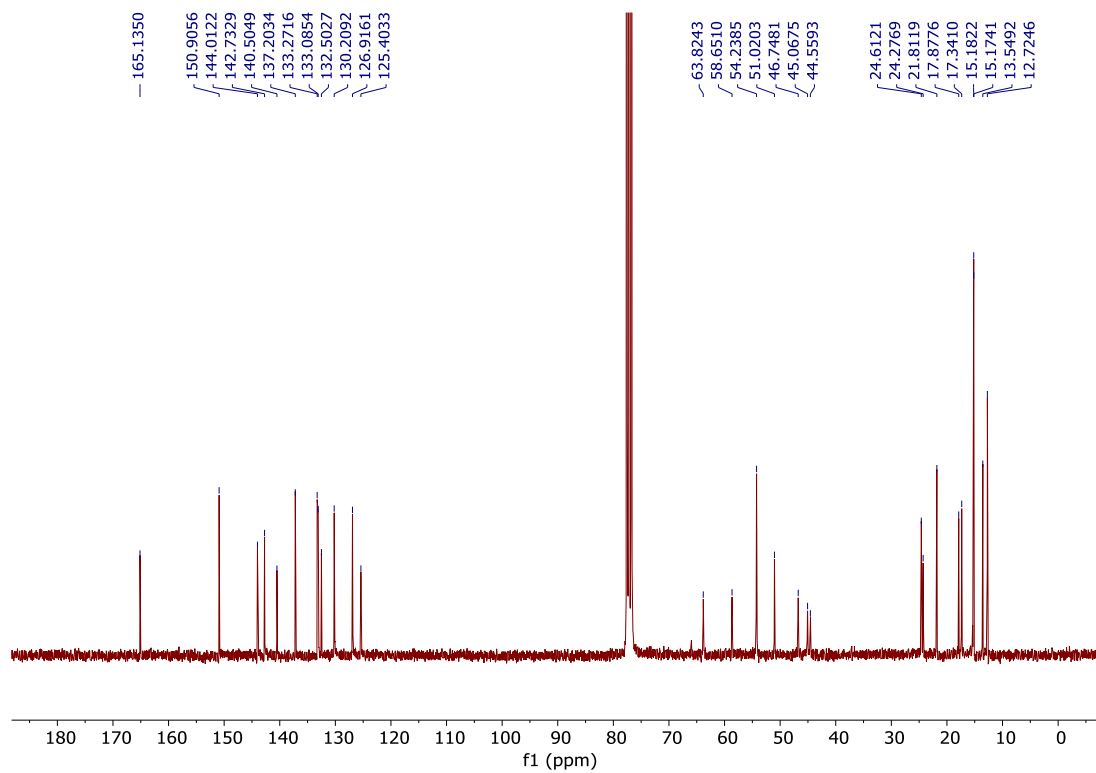
^{31}P NMR of NBDP-2 (121 MHz, CDCl_3):



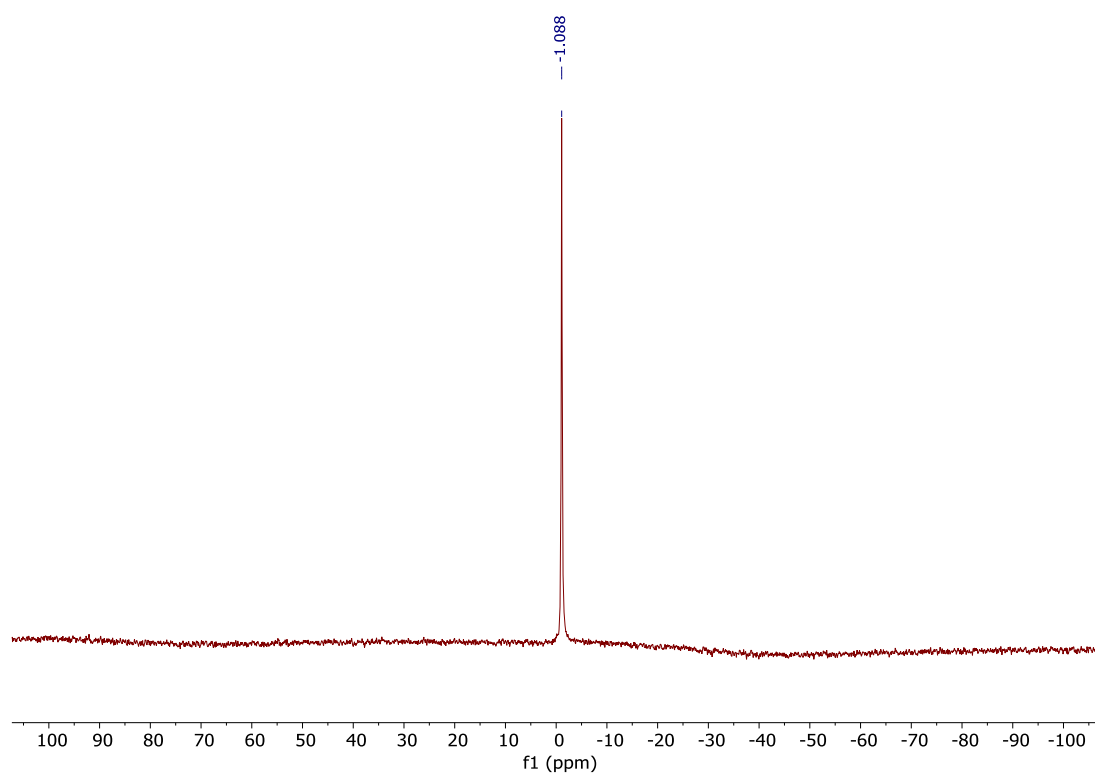
¹H NMR of NBDP-3 (300 MHz, CDCl₃):



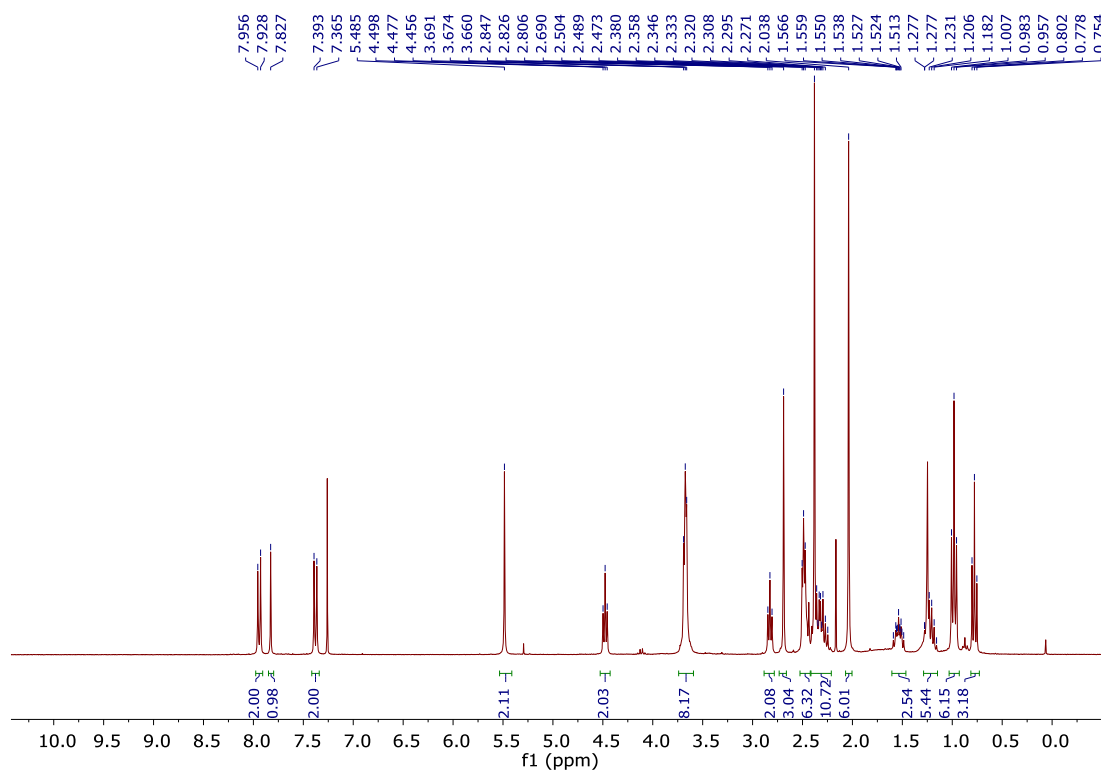
¹³C NMR of NBDP-3 (75 MHz, CDCl₃):



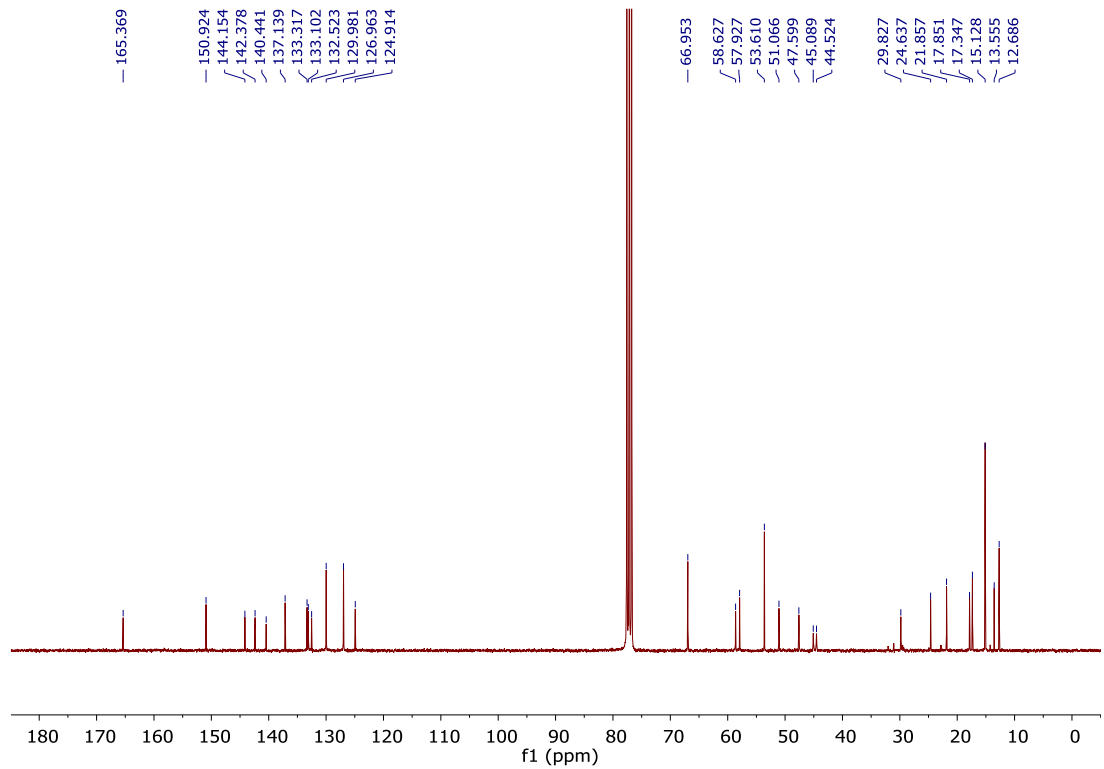
^{11}B NMR of NBDP-3 (160 MHz, CDCl_3):



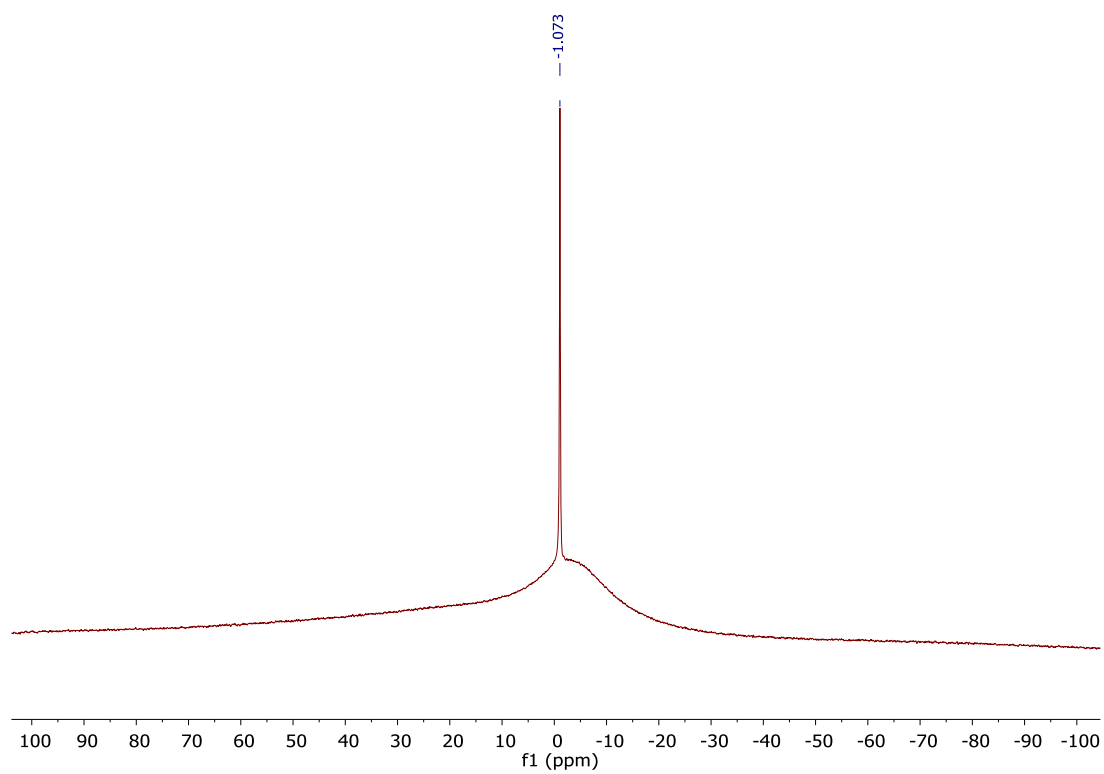
¹H NMR of NBDP-4 (300 MHz, CDCl₃):



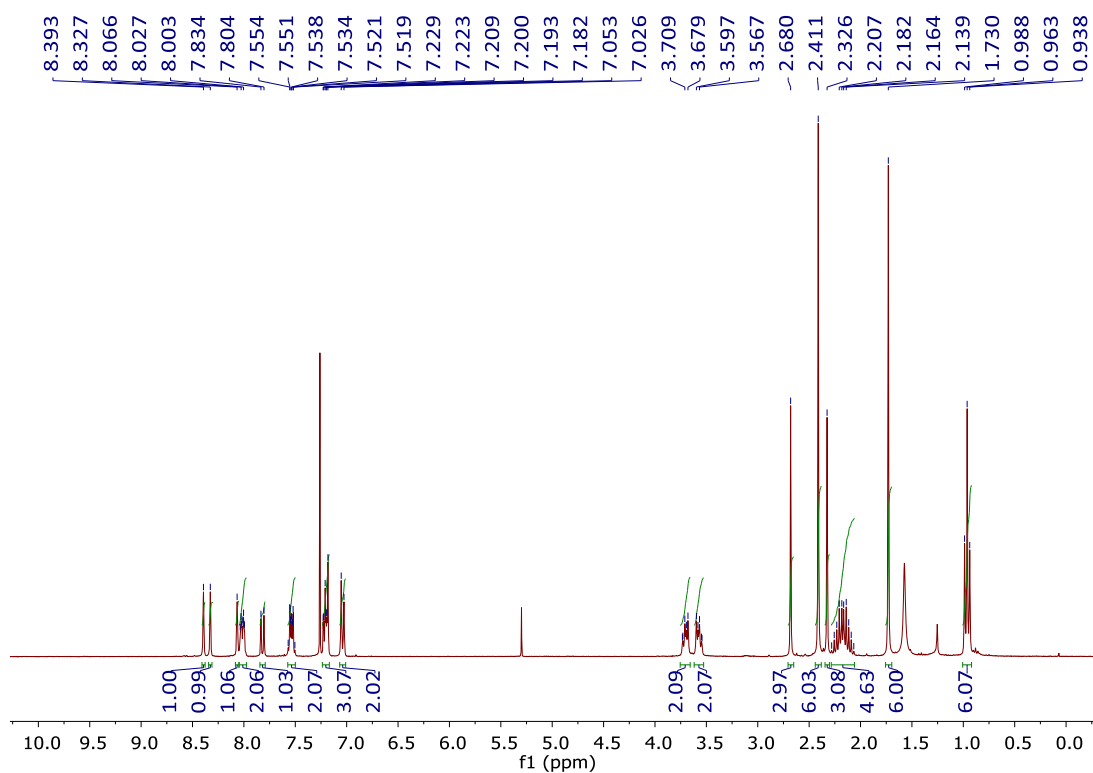
¹³C NMR of NBDP-4 (75 MHz, CDCl₃):



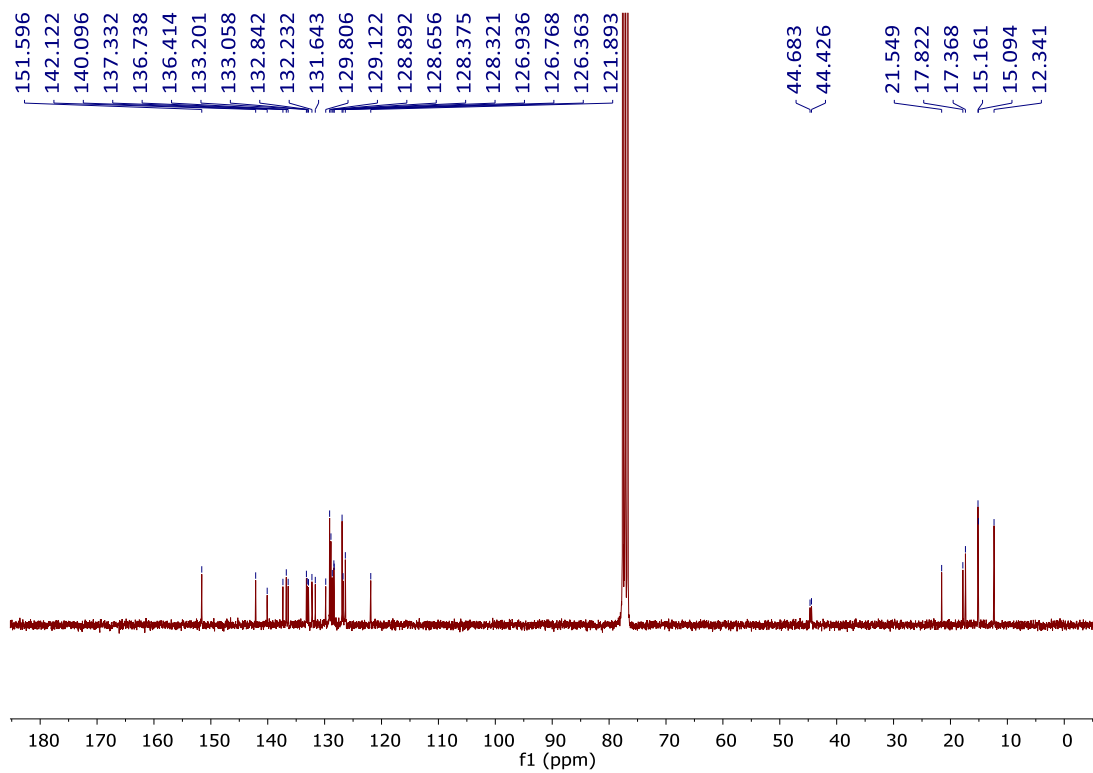
^{11}B NMR of NBDP-4 (160 MHz, CDCl_3):



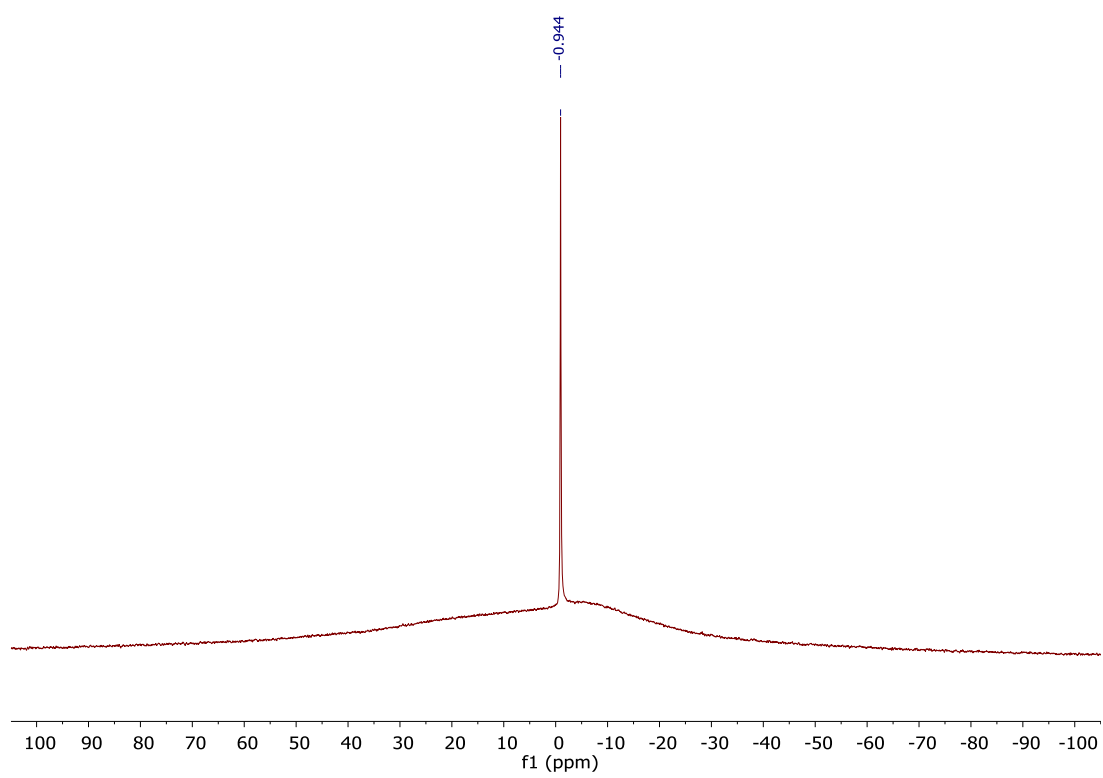
¹H NMR of NBDP-5 (300 MHz, CDCl₃):



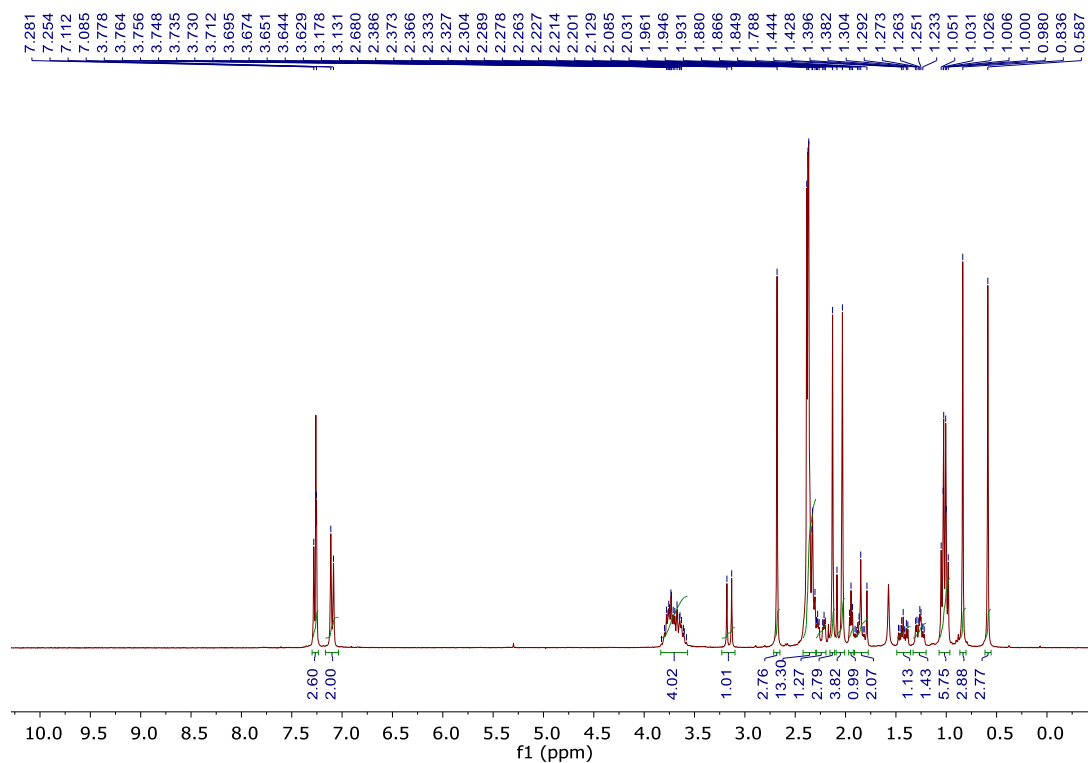
¹³C NMR of NBDP-5 (75 MHz, CDCl₃):



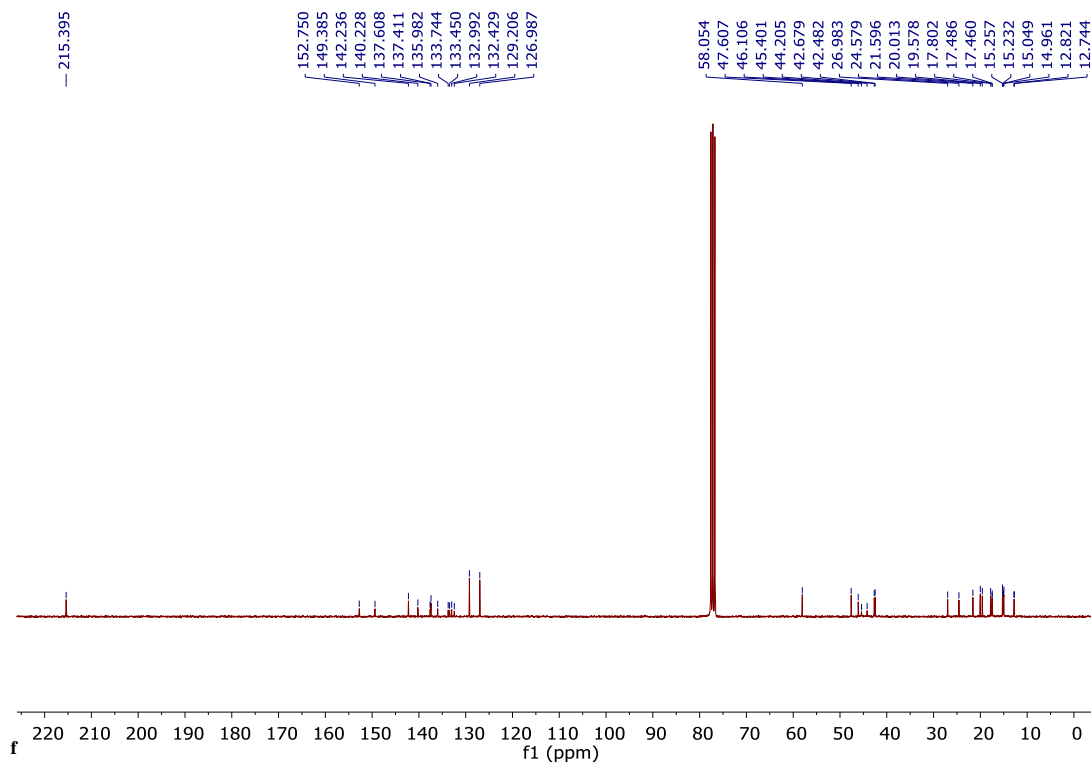
^{11}B NMR of NBDP-5 (160 MHz, CDCl_3):



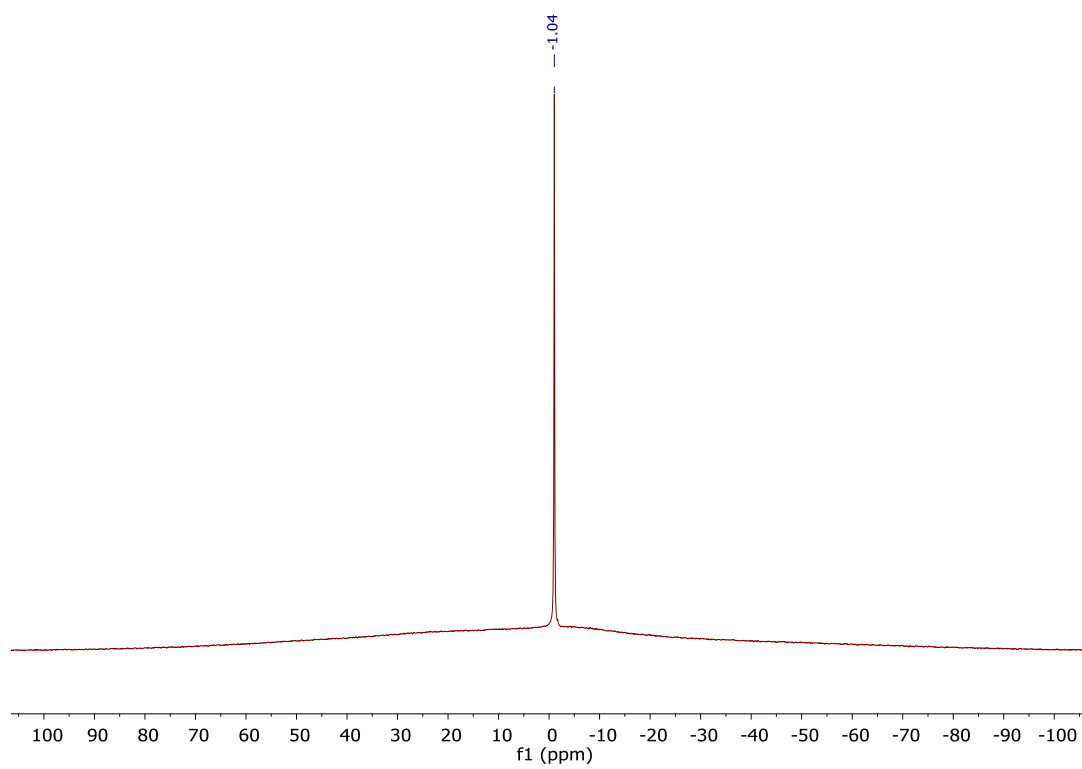
¹H NMR of NBDP-6 (300 MHz, CDCl₃):



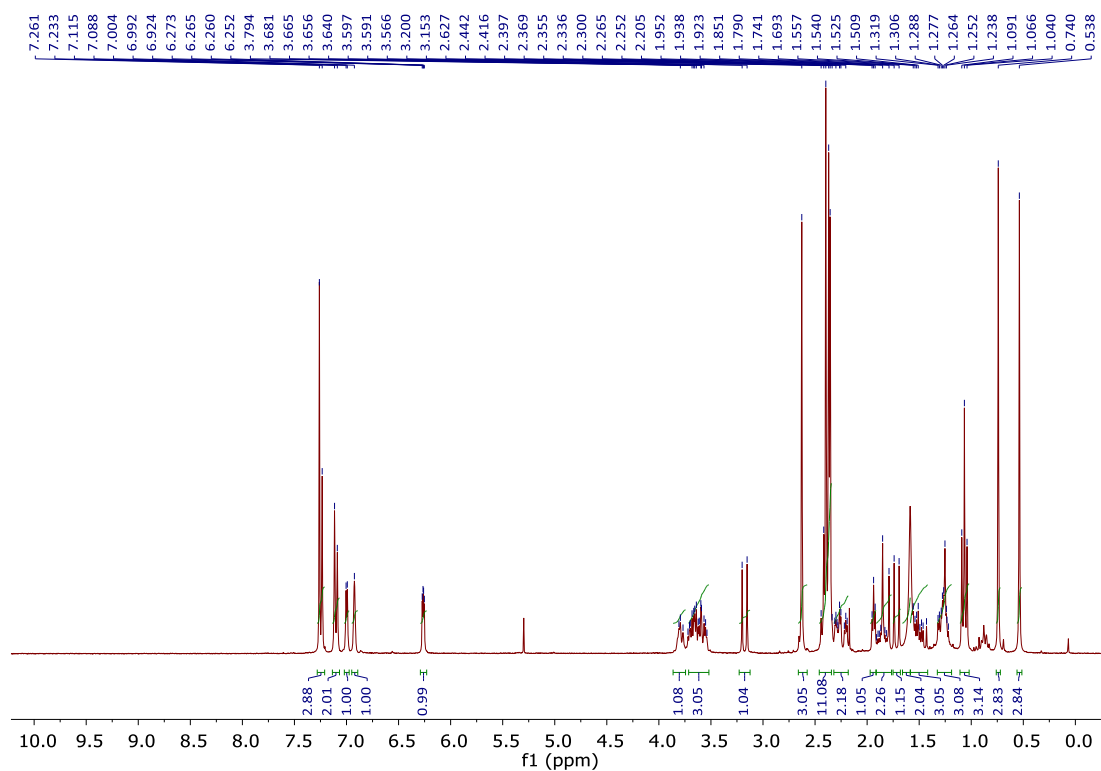
¹³C NMR of NBDP-6 (75 MHz, CDCl₃):



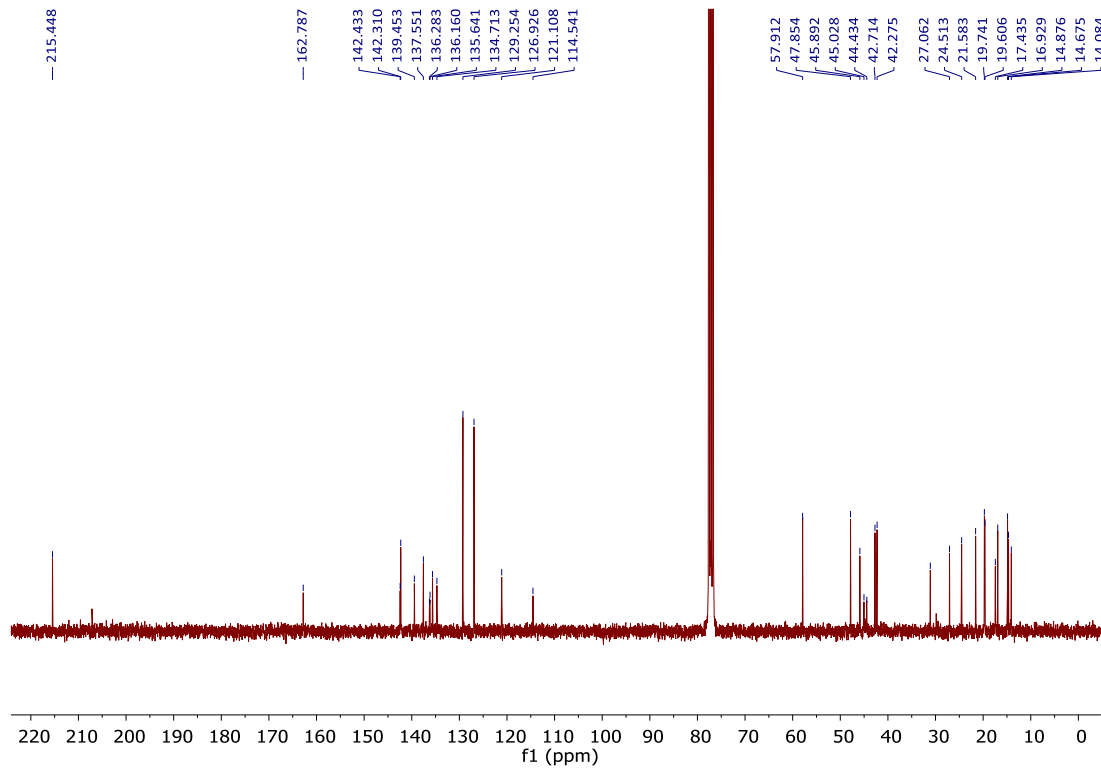
^{11}B NMR of NBDP-6 (160 MHz, CDCl_3):



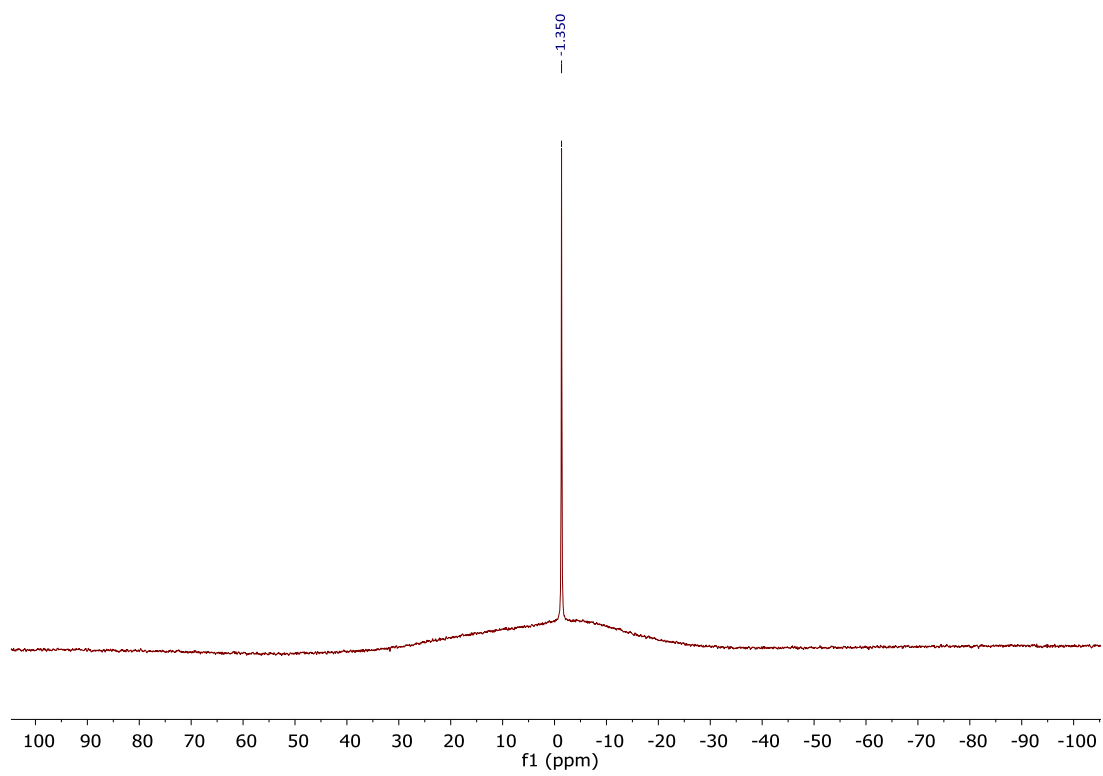
¹H NMR of NBDP-7-R (300 MHz, CDCl₃):



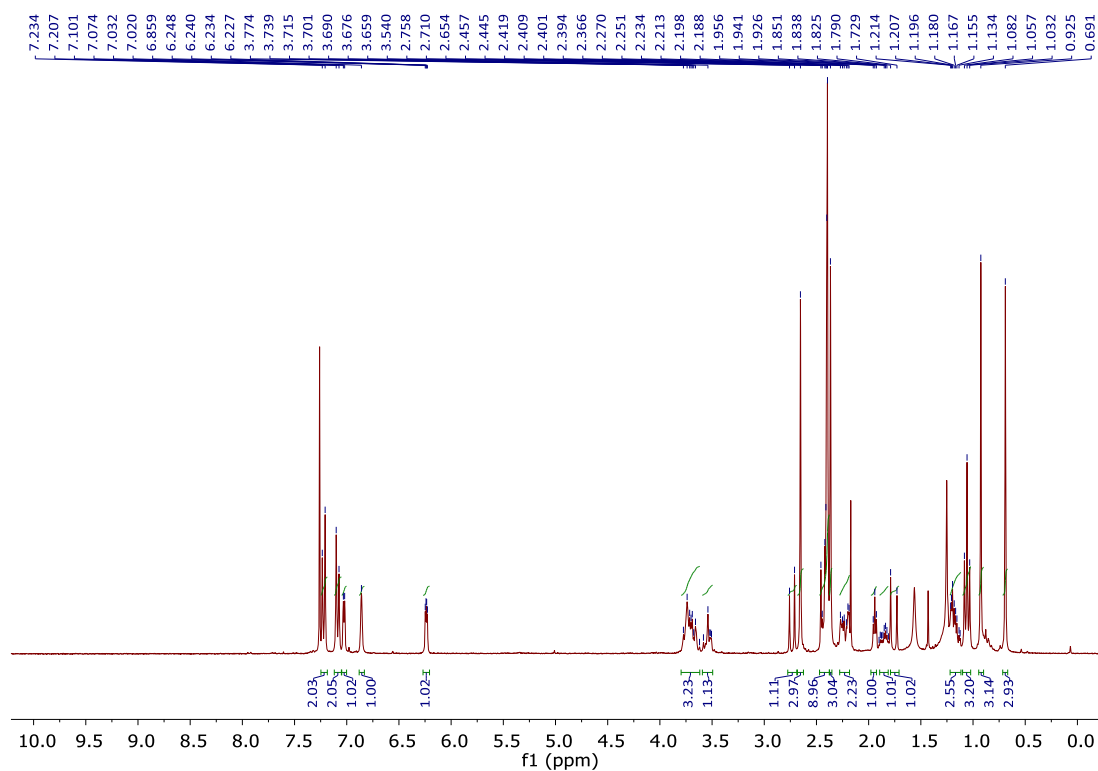
¹³C NMR of NBDP-7-R (75 MHz, CDCl₃):



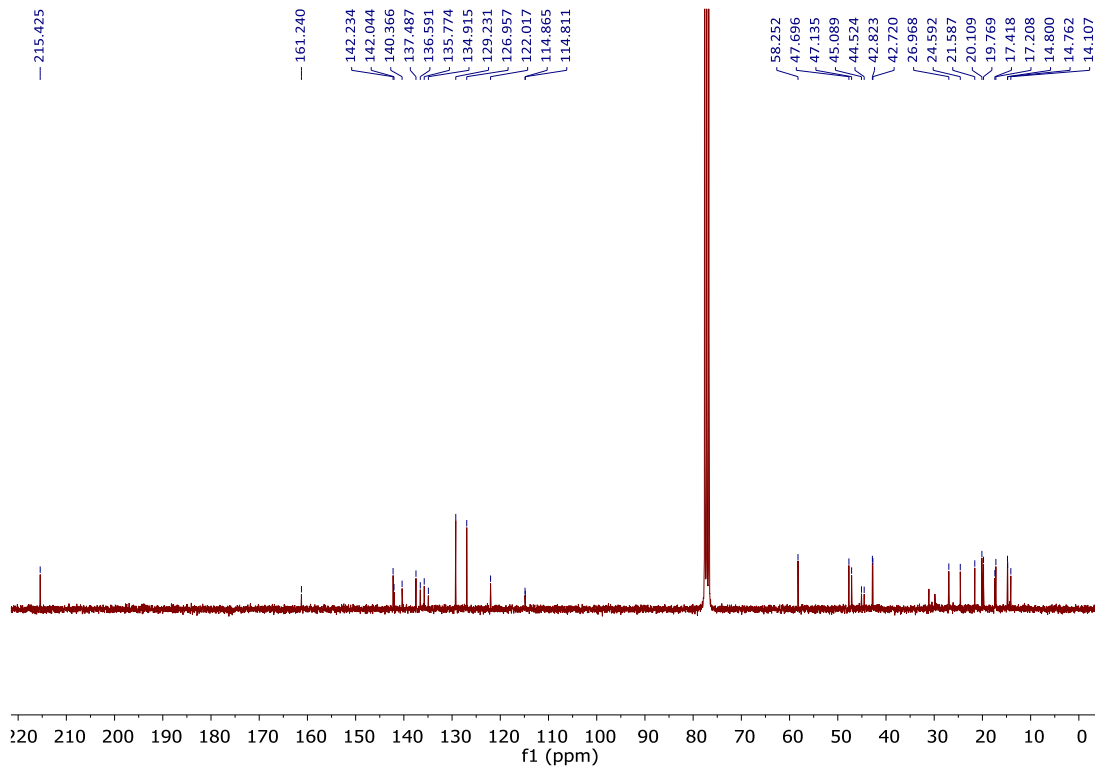
^{11}B NMR of NBDP-7-R (160 MHz, CDCl_3):



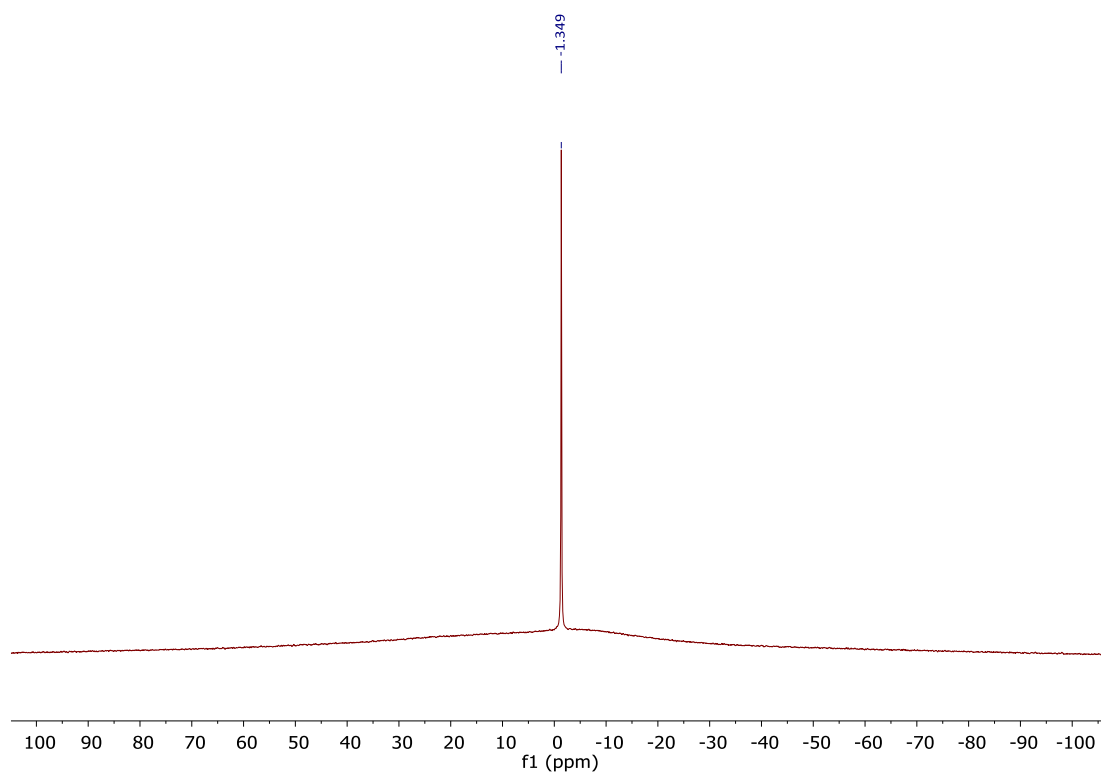
¹H NMR of NBDP-7-S (300 MHz, CDCl₃):



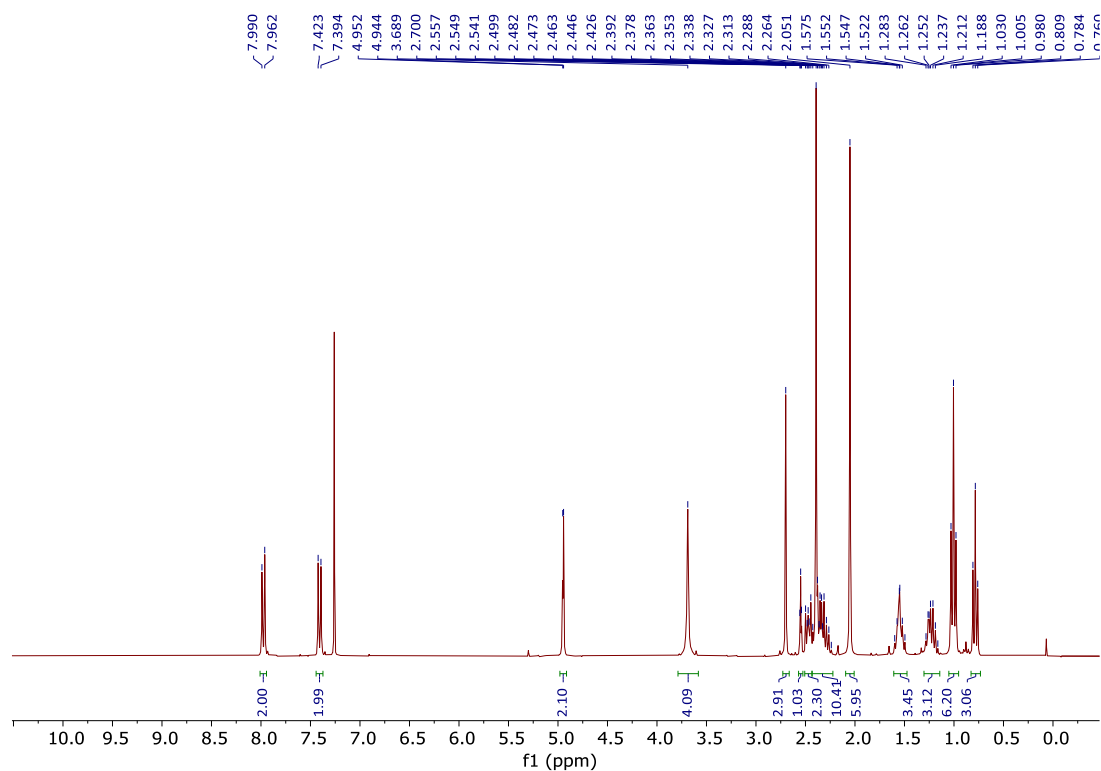
¹³C NMR of NBDP-7-S (75 MHz, CDCl₃)



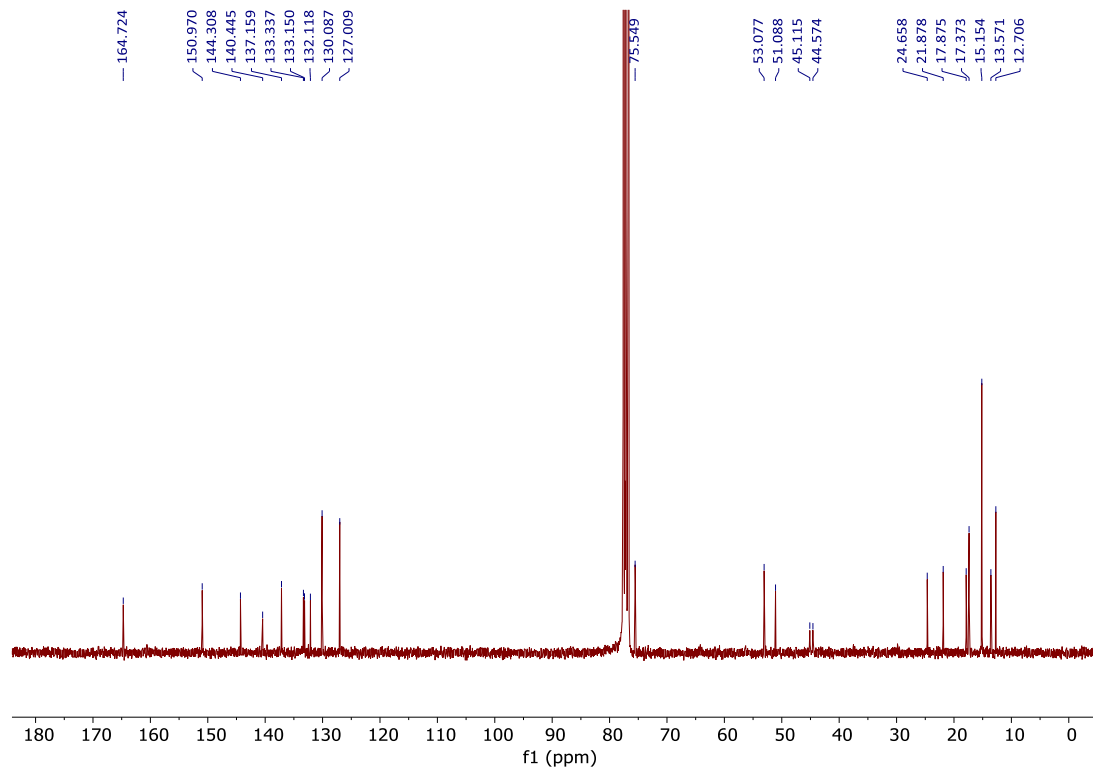
^{11}B NMR of NBDP-7-S (160 MHz, CDCl_3):



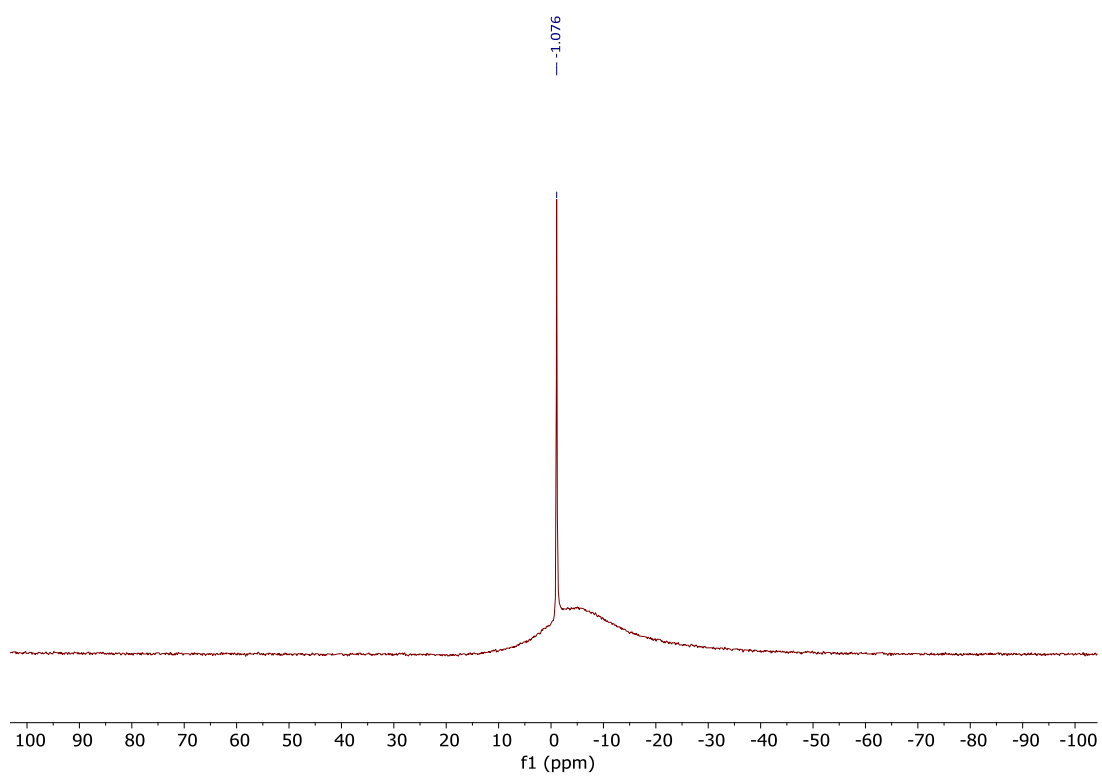
¹H NMR of NBDP-8 (300 MHz, CDCl₃):



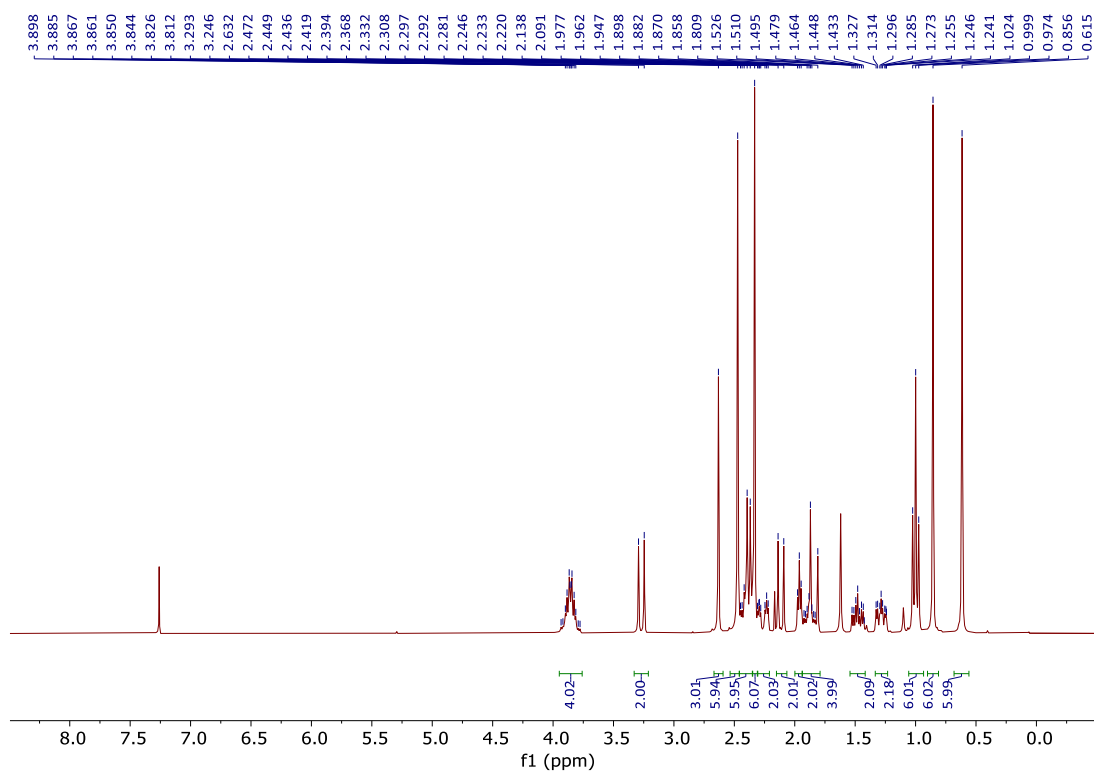
¹³C NMR of NBDP-8 (75 MHz, CDCl₃):



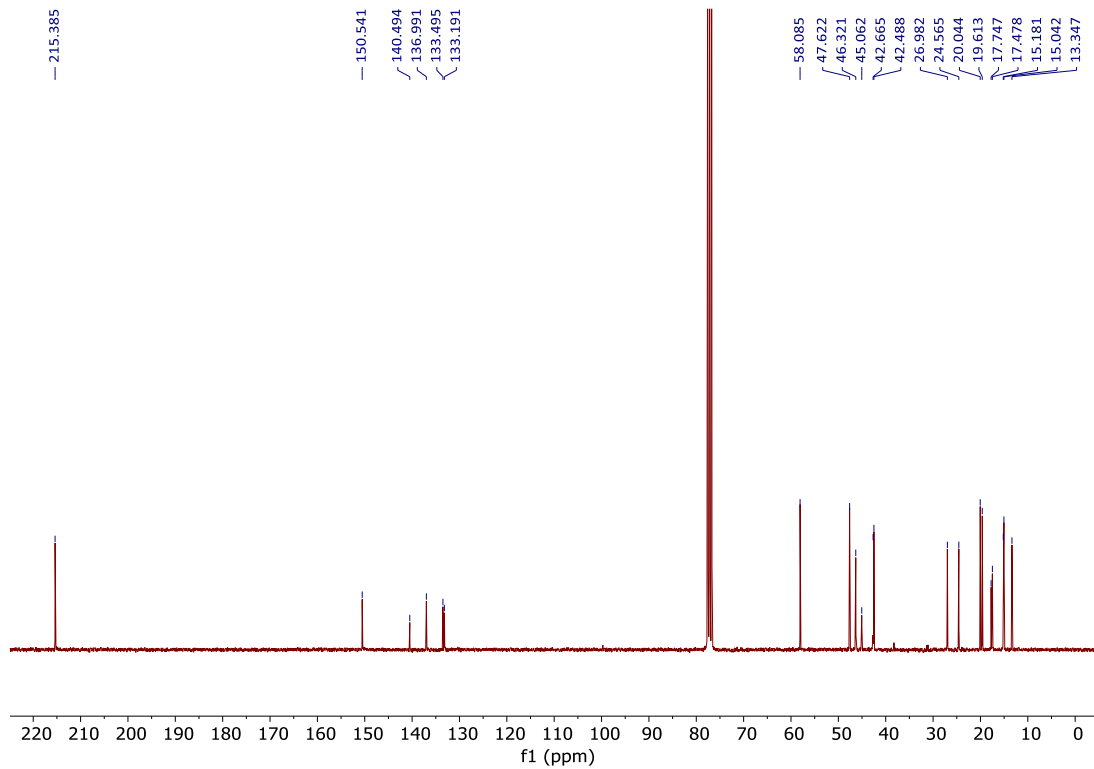
^{11}B NMR of NBDP-8 (160 MHz, CDCl_3):



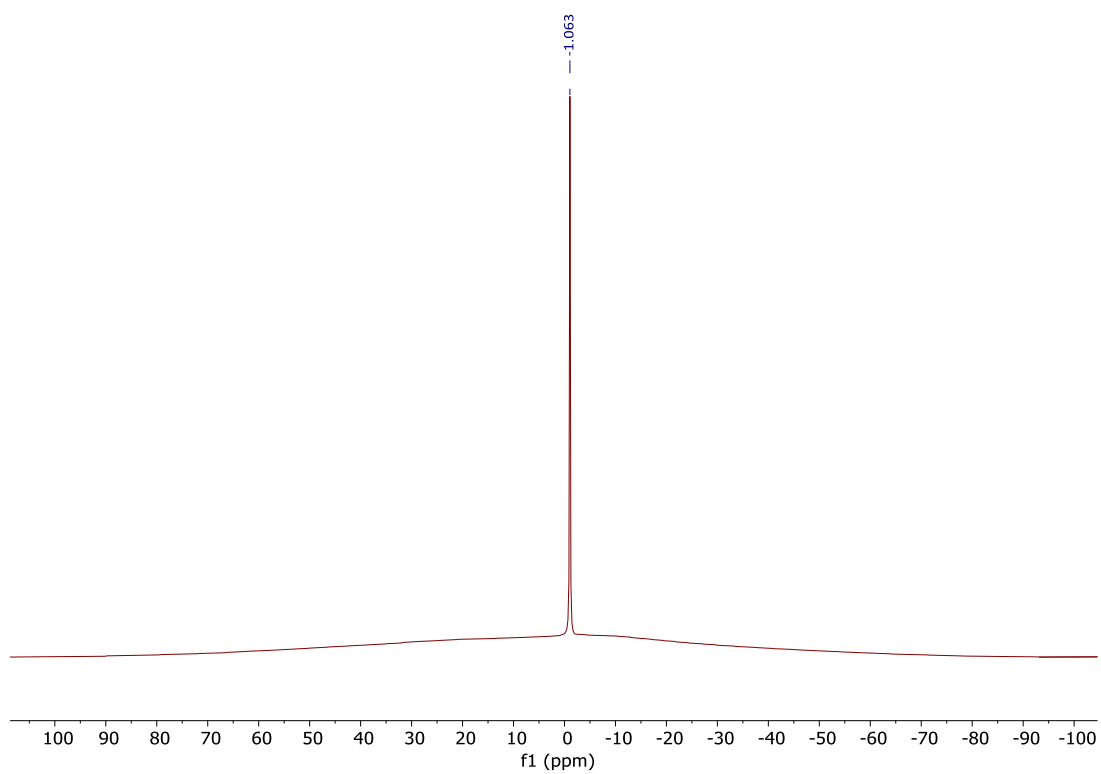
¹H NMR of NBDP-9 (300 MHz, CDCl₃):



¹³C NMR of NBDP-9 (75 MHz, CDCl₃):



^{11}B NMR of NBDP-9 (160 MHz, CDCl_3):



S4. Tables

Table S1. Ground visible photophysical signatures of new *N*-BODIPYs in different solvents (*ca.* 2×10^{-6} M) and precursor *F*-BODIPYs. Previously reported data for **NBDP-1** are included for comparison purposes.

Dye	Solvent	λ_{ab}^a (nm)	ϵ_{max}^b ($10^4 \times M^{-1}cm^{-1}$)	λ_{fl}^c (nm)	ϕ^d	τ^e (ns)
FBDP-1	<i>c</i> -hex	523.0	8.7	539.0	0.88	5.60
	EtOAc	517.0	7.6	533.0	0.84	5.78
	MeOH	516.0	7.4	534.0	0.81	6.10
NBDP-1^f	<i>c</i> -hex	529.0	7.0	544.5	0.94	7.14
	EtOAc	526.5	6.5	543.5	0.83	7.65
	MeOH	525.5	6.2	542.0	0.82	8.37
NBDP-2^{g,h}	MeOH	524.5	5.1	544.0	0.80	7.77
NBDP-3^{g,h}	MeOH	524.5	5.2	541.5	0.73	7.76
NBDP-4^g	EtOAc	525.0	4.7	545.5	0.80	7.49
	MeOH	524.5	5.5	543.5	0.88	7.82
NBDP-5	<i>c</i> -hex	527.0	6.6	545.5	0.85	6.84
	EtOAc	523.5	5.0	540.5	0.80	7.19
	MeOH	522.5	6.2	538.0	0.80	7.93
NBDP-6	<i>c</i> -hex	528.0	5.4	546.5	0.78	7.10
	CHCl ₃	527.5	5.6	543.5	0.88	7.22
	MeOH	524.0	5.6	541.5	0.82	8.31
NBDP-8	<i>c</i> -hex	528.5	5.3	547.5	0.80	7.09
	EtOAc	525.0	5.8	542.5	0.81	7.61
	MeOH	524.5	6.0	542.5	0.80	8.16
NBDP-9	<i>c</i> -hex	527.5	5.2	547.0	0.96	7.06
	EtOAc	524.0	5.6	542.0	0.90	7.58
	MeOH	523.0	5.5	542.0	0.93	8.28
FBDP-2	<i>c</i> -hex	503.5	5.7	514.5	0.93	5.52
	CHCl ₃	501.5	4.0	516.0	0.97	5.50
	MeOH	495.5	4.3	516.0	0.80	5.80
NBDP-7-R	<i>c</i> -hex	504.5	2.4	522.0	0.74	6.61
	CHCl ₃	504.5	2.7	520.0	0.85	6.88
	MeOH	502.5	2.6	519.5	0.87	8.00
NBDP-7-S	<i>c</i> -hex	506.5	2.6	522.0	0.71	6.26
	CHCl ₃	507.5	2.2	521.0	0.70	6.49
	MeOH	504.5	2.8	520.5	0.82	7.56

^aMaximum absorption wavelength. ^bMaximum molar absorption coefficient. ^cMaximum fluorescence wavelength. ^dFluorescence quantum yield. ^eFluorescence lifetime. ^fRef. S6; ^gThe dye is poorly soluble in *c*-hex. ^hThe dye is poorly soluble in EtOAc. *c*-hex: cyclohexane; EtOAc: ethyl acetate; MeOH: methanol.

Table S2. Maximum visible g_{abs} and g_{lum} values in CHCl₃ (*ca.* 2×10^{-5} and 1×10^{-3} , respectively) of chiral dissimilar-at-boron *N*-BODIPYs, and **NBDP-9**.

Dye	$10^3 \times g_{abs}^a$	$10^3 \times g_{lum}^b$
NBDP-6	-0.1	-0.8
NBDP-7-R	+1.4	+0.4
NBDP-7-S	-1.2	-0.8
NBDP-9	0.0	+1.0

^aKunh's dissymmetry ratio; ^bLuminescence dissymmetry factor.

Table S3. Crystallographic data for **NBDP-7-R**.

formula	C ₃₃ H ₄₃ B ₁ N ₄ O ₅ S ₂
formula weight	650.64
crystal system	hexagonal
space group	P6 ₁
a (Å)	18.0361 (3)
b (Å)	18.0361 (3)
c (Å)	21.5141 (4)
α (deg)	90
β (deg)	90
γ (deg)	120
V (Å ³)	6060.92 (16)
Z	6
Dc (g·cm ⁻³)	1.070
F(000)	2076.0
Data/restraints/parameters	7475/87/347
Goodness of Fit on F ²	1.377
R1 (I > 2σ(I))	0.1174
wR2 (all data)	0.3395

S5. Figures

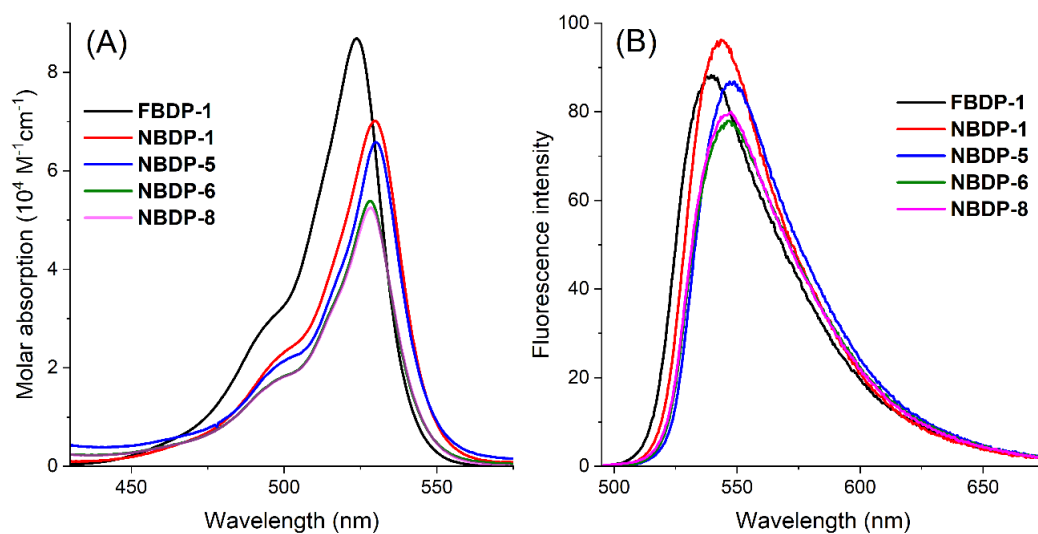


Fig. S1. Absorption (A) and fluorescence (B, scaled by their efficiency) spectra of **FBDP-1** (PM567) and PM567-based dissimilar-at-boron *N*-BODIPYs **NBDP-1**, **NBDP-5**, **NBDP-6** and **NBDP-8** in cyclohexane (*ca.* 2×10^{-6} M).

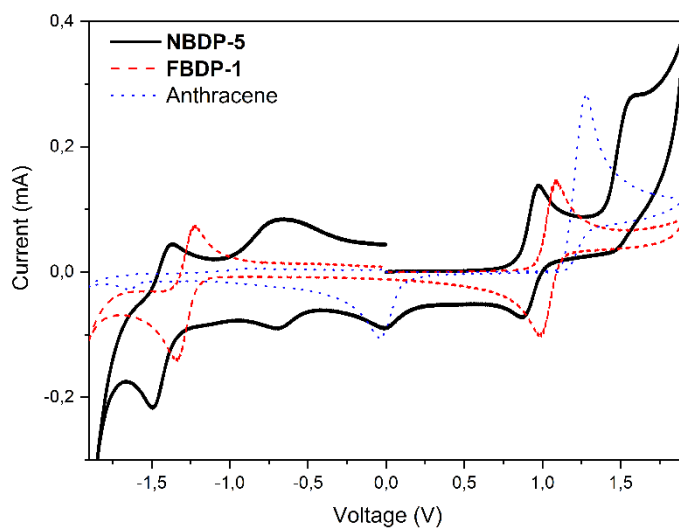


Fig. S2. Cyclic voltammogram of **NBDP-5** (black, bold) and its corresponding isolated chromophoric units: *F*-BODIPY **FBDP-1** (red, dotted) and anthracene (blue, dotted), in acetonitrile.

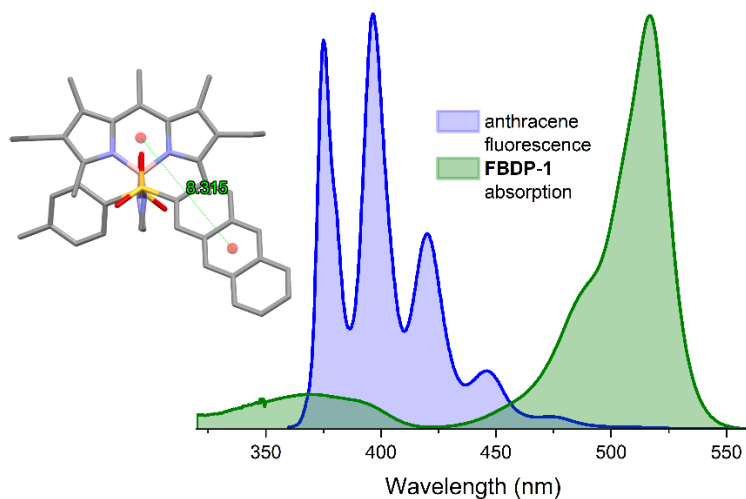


Fig. S3. Normalized fluorescence spectrum of anthracene (blue) and UV-Vis absorption spectrum of **FBDP-1** (green) in cyclohexane. The ground state optimized geometry (B3LYP/6-311g*) of **NBDP-5** is also enclosed to highlight the mutual orientation and distance between the acting chromophores (*ca.* 8.3 Å) in the molecular array.

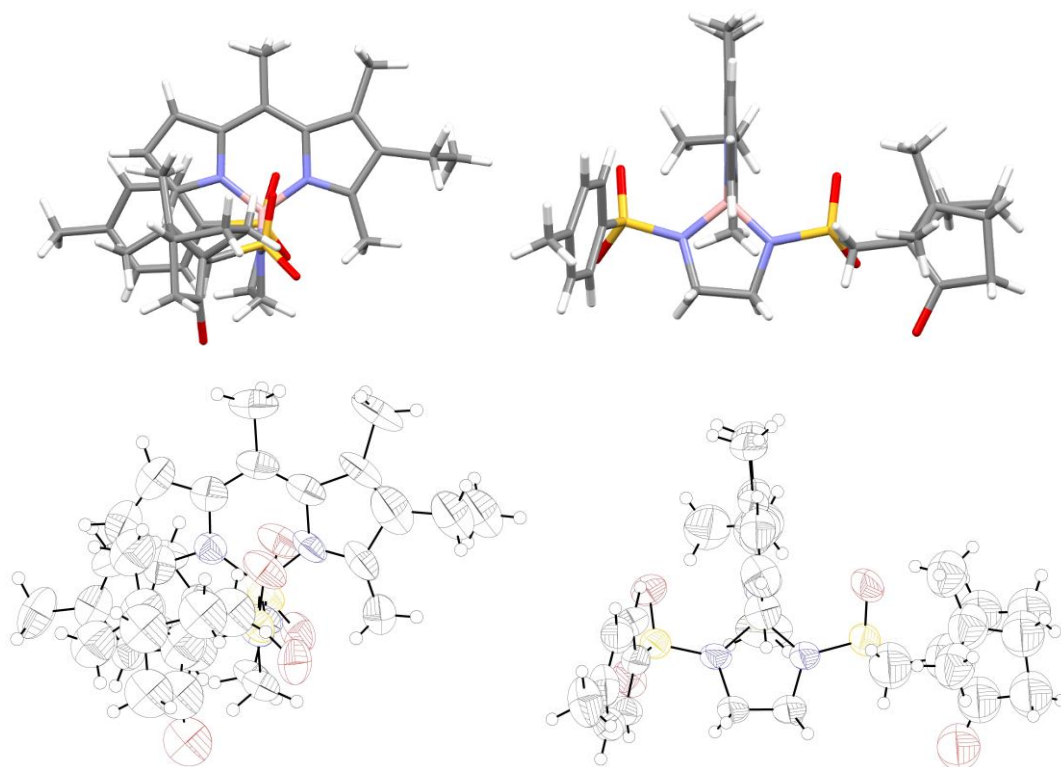


Fig. S4. Molecular structure (top, sticks; bottom, ORTEP) of **NBDP-7-R** determined by X-ray diffraction in frontal view (left) and side view (right).

S6. References

- S1. H. P. J. M. Dekkers, P. F. Moraal, J. M. Timper, J. P.; Riehl, *Appl. Spectrosc.*, 1985, **39**, 818.
- S2. Bolte, F. P. Cordelières, *J. Microsc.*, 2006, **224**, 213-232.
- S3. C. Ray, A. García-Sampedro, C. Schad, E. Avellanal-Zaballa, F. Moreno, M. J. Ortiz, J. Bañuelos, A. Villanueva, P. Acedo, B. L. Maroto and S. de la Moya, *Chem. Proc.*, 2021, **3**, 15.
- S4. S. St John-Campbell, A. J. P. White and J. A. Bull, *Chem. Sci.*, 2017, **8**, 4840-4847.
- S5. J. Bañuelos, I. Lopez-Arbeloa, I. García-Moreno, A. Costela, L. Infante, E. Perez-Ojeda, M. Palacios-Cuesta and M. J. Ortiz, *Chem. Eur. J.*, 2010, **16**, 14094-14105.
- S6. C. Ray, L. Díaz-Casado, E. Avellanal-Zaballa, J. Bañuelos, L. Cerdán, I. García-Moreno, F. Moreno, B. L. Maroto, Í. López-Arbeloa and S. de la Moya, *Chem. Eur. J.*, **2017**, *23*, 9383-9390.